

REC'D OCT 24 1946

CLASSIFICATION CANCELLED

CONFIDENTIAL

RM No. L6118

CLASSIFICATION CANCELLED

1136.3
Republic F-12

Authority *H. L. Dryden*
Dir., Aeron. Research
NACA

NACA 10-1-52

By *oef*

See *NACA change*
#968

RESEARCH MEMORANDUM

for the

Air Materiel Command, Army Air Forces

CHARACTERISTICS OF A SEALED INTERNALLY BALANCED AILERON
FROM TESTS OF A $\frac{1}{4}$ -SCALE PARTIAL-SPAN MODEL OF THE
REPUBLIC XF-12 AIRPLANE IN THE LANGLEY 19-FOOT
PRESSURE TUNNEL

By

Robert R. Graham, Albert P. Martina, and Reino J. Salmi

Langley Memorial Aeronautical Laboratory
Langley Field, Va.

CONTAINS PROPRIETARY
INFORMATION

ALL INFORMATION CONTAINED
HEREIN IS UNCLASSIFIED
DATE 11-1-46 BY 1136.3

FILE COPY
To be placed in
the files of the
to the
Washington, D. C.

**NATIONAL ADVISORY COMMITTEE
FOR AERONAUTICS**

WASHINGTON

11-1-46

CLASSIFICATION CANCELLED

CONFIDENTIAL

CONFIDENTIAL
CLASSIFICATION CANCELLED

NATIONAL ADVISORY COMMITTEE FOR AERONAUTICS

RESEARCH MEMORANDUM

for the

Air Materiel Command, Army Air Forces

CHARACTERISTICS OF A SEALED INTERNALLY BALANCED AILERON

FROM TESTS OF A $\frac{1}{4}$ -SCALE PARTIAL-SPAN MODEL OF THE

REPUBLIC XF-12 AIRPLANE IN THE LANGLEY 19-FOOT

PRESSURE TUNNEL

By Robert R. Graham, Albert P. Martina, and Reino J. Salmi

SUMMARY

An investigation was conducted on a $\frac{1}{4}$ -scale partial-span model of the Republic XF-12 airplane to determine its aileron and aileron-tab characteristics. The effects of wing roughness and aileron balance-seal leakage on the aileron and tab characteristics were also investigated. The model was tested at several angles of attack and flap deflections through a range of aileron and aileron-tab deflections. The Reynolds and Mach numbers for the tests were 8,600,000 and 0.17, respectively.

The results of the tests indicated that at small aileron and tab deflections: (a) the rate of change of aileron hinge-moment coefficient with aileron deflection had a positive value at low angles of attack with flaps neutral but as the angle of attack was increased or the flaps were deflected, the value decreased until at high angles of attack with flaps neutral or moderate angles of attack with flaps deflected it became negative; this condition indicates the need for reducing the balancing effect to prevent illogical control wheel forces at high speeds; (b) at all flap deflections the rate of change of aileron hinge-moment coefficient with angle of attack varied from positive values at low angles of attack to negative values at high angles of attack; (c) at conditions simulating high-speed flight, wing roughness tended to further increase the positive value of the rate of change of aileron hinge-moment coefficient with aileron deflection but reduced the rate of change of rolling-moment coefficient with aileron deflection; and (d) increasing the balance-seal leakage decreased the rate of change of both aileron hinge-moment coefficient and rolling-moment coefficient with aileron deflection but had a negligible effect

CONFIDENTIAL
CLASSIFICATION CANCELLED

on the rate of change of aileron hinge-moment coefficient with tab deflection.

INTRODUCTION

The XF-12 is a high speed, high altitude, long range, photographic airplane designed by the Republic Aviation Corporation for the Army Air Forces. It is of conventional design and is powered by four Pratt & Whitney R-4360 engines. The over-all dimensions and some of the details of the airplane are shown in figure 1. To aid in the design, models of several components of the airplane were tested in various wind tunnels of the NACA Langley Laboratory.

One of the models was a $\frac{1}{4}$ -scale partial-span model of the left wing of the airplane. It was tested in the Langley propeller research tunnel in the development of the wing duct inlets to be used on the airplane and in the Langley 19-foot pressure tunnel to obtain an indication of the effects of the wing duct inlets on the maximum lift and stalling characteristics of the model and to determine the aileron and aileron-tab characteristics of the model.

This paper presents the results of the aileron investigation and includes rolling-moment, yawing-moment, and aileron hinge-moment coefficients and pressure coefficients across the aileron-balance seal through a range of angle of attack, tab deflection, and aileron deflection with flaps neutral and deflected 20° and 55° . Some of the effects of wing roughness and balance seal leakage on the aileron and tab characteristics are also presented.

SYMBOLS AND COEFFICIENTS

The symbols and coefficients presented in this report are defined as follows:

- C_L lift coefficient (L/qS)
- C_D drag coefficient (D/qS)
- C_Y lateral-force coefficient (Y/qS)
- C_m pitching-moment coefficient ($M/qc'S$)

- C_l rolling-moment coefficient (L^*/q_bS)
- C_n yawing-moment coefficient (N/q_bS)
- C_{h_a} aileron hinge-moment coefficient $\left(\frac{H_a}{q b_a \bar{c}_a^2} \right)$
- ΔP pressure coefficient across internal balance
(pressure below balance minus pressure above balance divided by free stream dynamic pressure)
- E leakage factor $\left(1 - \frac{P(b) - P(c)}{P(a) - P(d)} \right)$
- $P(b) - P(c)$ pressure difference across balance of internal balance
- $P(a) - P(d)$ applied pressure difference across vents of internal balance
- F overhang factor for complete aileron

$$\left[\left(\frac{\bar{c}_b}{\bar{c}_a} \right)^2 - \left(\frac{\frac{t}{2}}{\bar{c}_a} \right)^2 \right] \frac{b_b}{b_a}$$
- F_1 overhang factor for inboard balance chamber

$$\left[\left(\frac{\bar{c}_{b1}}{\bar{c}_a} \right)^2 - \left(\frac{\frac{t_1}{2}}{\bar{c}_a} \right)^2 \right] \frac{b_{b1}}{b_a}$$
 (corresponding for outboard chamber F_2)
- q free-stream dynamic pressure $\left(\frac{1}{2} \rho V^2 \right)$
- ρ mass density of air
- V velocity of air in free stream
- L lift
- D drag
- Y lateral force

M	pitching moment about airplane center-of-gravity location (0.2743 c ³ on fuselage center line)
L ^r	rolling moment about airplane center-of-gravity location
N	yawing moment about airplane center-of-gravity location
H _a	aileron hinge moment
S	wing area
c ²	wing mean aerodynamic chord
b	wing span
\bar{c}_a	root-mean-square chord of aileron behind hinge axis
\bar{c}_b	root-mean-square chord of balance from aileron hinge axis to middle of sealed gap
b _a	aileron span
b _b	balance span
\bar{t}	root-mean-square thickness of aileron at hinge axis
α	angle of attack of wing root chord
δ_f	flap deflection
δ_a	aileron deflection with respect to wing, positive with trailing edge down
δ_t	aileron tab deflection with respect to aileron, positive with trailing edge down
R	Reynolds number $\left(\frac{\rho V c^2}{\mu} \right)$
M	Mach number (V/a)
μ	coefficient of viscosity
a	velocity of sound

Subscripts:

1 inboard balance chamber

2 outboard balance chamber

Slopes:

$$C_{n_{a\delta_a}} = \left(\frac{\partial C_{n_a}}{\partial \delta_a} \right)_{\alpha, \delta_t}$$

$$C_{n_{a\alpha}} = \left(\frac{\partial C_{n_a}}{\partial \alpha} \right)_{\delta_a, \delta_t}$$

$$C_{n_{a\delta_t}} = \left(\frac{\partial C_{n_a}}{\partial \delta_t} \right)_{\alpha, \delta_a}$$

$$C_{l_{\delta_a}} = \left(\frac{\partial C_l}{\partial \delta_a} \right)_{\alpha, \delta_t}$$

$$(\Delta P)_{\delta_a} = \left[\frac{\partial (\Delta P)}{\partial \delta_a} \right]_{\alpha, \delta_t}$$

where subscripts to the partial derivatives indicate factors held constant.

MODEL AND APPARATUS

The $\frac{1}{4}$ -scale partial-span model of the Republic XF-12 airplane represents the outboard 92.4 percent of the left wing of the airplane. The principal dimensions of the model are shown in figure 2 and table I. The airfoil sections were developed by the Republic company and are described in reference 1.

The model was tested in the Langley 19-foot pressure tunnel in conjunction with a reflection plane. (See reference 2.) The general dimensions of the tunnel setup are shown in figure 3 and views of the model in the tunnel are shown in figure 4. The gap between the inboard end of the model and the reflection plane was maintained at $3/16 \pm 1/32$ inch by means of an automatic telescoping mechanism built into the model.

The model was equipped with a sealed internally balanced aileron, the dimensions of which are shown in figures 5 and 6. The gaps between the leading edge of the balance and the forward wall of the balance compartment and between the ends of the balance and the sides of the hinges were sealed with flexible, koroseal impregnated voile. The deflection of the aileron was remotely controlled by means of a hydraulic piston which was connected to the aileron through a beam upon which electrical strain gages were mounted for measuring the hinge moments. The aileron deflections were remotely indicated by a potentiometer type control position indicator which was connected directly to the aileron. The aileron

was equipped with a manually adjustable constant chord tab whose leading-edge gap was sealed by a rubber wiper seal. No provision was made for measuring the tab hinge moments.

The flaps on the model were of the double-slotted type and were mounted by means of brackets which fixed them at the desired deflections. The general arrangement of the flaps is shown in figure 7. The angles of deflection tested were neutral, 20° , and 55° .

An air inlet which was developed in the Langley propeller research tunnel was installed along the leading edge of the wing between the nacelles. The inlet was connected to ducts which represented the intercooler, the oil cooler, and the charge air ducts of the airplane. The ducts had exits along the lower surfaces of both nacelles and were equipped with adjustable shutters for regulating the air flow. The shutters were set to give ratios of velocity in the duct entrance to velocity in the free stream of 0.41 at 2° angle of attack, with flaps neutral to simulate the high-speed condition and 0.75 at 8° angle of attack with flaps deflected 20° and 55° to simulate the take-off and landing-approach conditions.

The shutters were not changed for other angles of attack. The cowl exit flaps were set to simulate the airplane cruising condition for all tests.

For some tests with flaps neutral a roughness strip was installed on the upper and lower surfaces of the wing at 0.20c. Calculations indicated that transition at that location on the model would cause the relative thickness of the boundary layer over the aileron to be approximately the same as that on the airplane at high speed with transition at the leading edge of the wing. The roughness strip was obtained by application of number 60 (0.011-inch diameter) carborundum grains to a thin layer of shellac about $\frac{1}{2}$ -inch wide and extending along the full span of the model. The grains covered 5 to 10 percent of the area of the strips.

To obtain an indication of the effects of seal leakage on the aileron characteristics, some tests were made with a series of $\frac{1}{4}$ -inch holes drilled in the balance near its leading edge. The holes were evenly spaced along the span of the balance with an equal number of holes in each compartment. The leakage factors for the seal, with and without the holes, were determined by placing a rectangular box over the upper surface vent and applying air pressure to the box. The leakage factors were determined for applied pressure differences ranging from 10 to 100 pounds per square foot

for the "no hole" condition and 10 to 60 pounds per square foot for the maximum leakage condition. The leakage factors thus obtained are presented in figure 8. The leakage factors showed no definite trend with variation of pressure across the vents so the curves of figure 8 represent an average of the values obtained.

TESTS

The aileron and tab characteristics were determined by measuring the rolling moments, yawing moments, and aileron hinge moments at several angles of attack through a range of tab and aileron deflection. Balance compartment pressures were also measured for the tab neutral condition. The characteristics were determined with the double-slotted flaps neutral and deflected 20° and 55° . The effects of the roughness strips and leakage holes on the aileron characteristics were determined only for the flap neutral condition.

The lift, drag, and pitching-moment characteristics of the model were determined through a range of angle of attack with the aileron and tab neutral and with the flaps neutral and deflected 20° and 55° .

The tests were made at a value of dynamic pressure of approximately 100 pounds per square foot with the air in the tunnel compressed to approximately $2\frac{1}{4}$ atmospheres. The Reynolds and Mach numbers thus obtained were 8,600,000 and 0.17, respectively.

CORRECTIONS TO DATA

The results of all tests have been reduced to standard nondimensional coefficient form so that they apply to a complete span wing with 6° dihedral. Moments were computed about a point corresponding to a center-of-gravity location on the center line of the airplane fuselage at 27.43 percent of the mean aerodynamic chord.

Jet-boundary corrections and plan-form corrections were calculated and applied to the data by the method described in reference 2. Corrections for the absence of dihedral in the model were made by rotating the axes of the forces and moments 6° (the amount of dihedral on the airplane) and by correcting the projected model area and span for the effects of rotation.

The total corrections applied are as follows:

$$C_L = C_{L_{gross}} - 0.1051 C_{V_{gross}}$$

$$C_D = 1.0055 C_{D_{gross}} + 0.0154 C_{L_{gross}}^2$$

$$C_m = C_{m_{gross}} + 0.0087 C_{L_{gross}} - 1.8685 C_{n_{gross}}$$

$$C_l = 0.8012 (C_{l_{gross}} - C_{l_{tare}})$$

$$C_n = 1.0055 (C_{n_{gross}} - C_{n_{tare}}) + (-0.0311 C_l C_{L_{gross}}) + 0.0059 C_{m_{gross}}$$

$$\alpha = \alpha_{tunnel} + 1.003 C_{l_{gross}}$$

where the subscript "gross" refers to the uncorrected coefficient and the subscript "tare" refers to the uncorrected coefficient obtained with aileron and tab neutral. The tare and interference effects of the model supports have been neglected because of the difficulties involved in their determination. The influence of these effects on the aileron characteristics, however, is believed to be small.

RESULTS AND DISCUSSION

The results of the aileron tests are presented in figures 9 to 20 and are summarized in table II. The lift, drag, and pitching-moment characteristics of the model are presented in figure 21.

Smooth model aileron and tab characteristics.- The characteristics of the sealed aileron on the smooth model with the double-slotted flaps neutral and deflected 20° and 55° are presented in figures 9 to 13. The parameters of table II obtained from these figures show that at low angles of attack with flaps neutral $C_{ha\delta_a}$ is positive through a limited range of deflections. As the angle of attack is increased or the flaps are deflected $C_{ha\delta_a}$ decreases until at large angles of attack with flaps neutral or moderate angles of attack with flaps deflected it becomes negative. Table II also shows that $C_{ha\alpha}$ is positive at low angles of attack and becomes negative at angles of attack above 6° with all flap deflections. The reversal of sign of $C_{ha\delta_a}$ indicates that the

that the control wheel forces for a direct linked aileron on the airplane would be in the logical direction at low and moderate speeds but in the illogical direction at high speeds. The sign of $C_{h_{a\alpha}}$ is such that it tends to relieve the overbalanced condition in the high-speed range of angles of attack and the underbalanced condition in the low-speed range of angles of attack when the airplane is in a steady roll.

Effects of roughness on aileron and tab characteristics.- The effects of upper and lower surface roughness strips at 0.20c on the flap neutral aileron and tab characteristics are shown in figures 14, 15, and 16. At the lower angle of attack investigated ($\alpha = 0.8^\circ$) the roughness strips caused an increase in $C_{h_{a\delta_a}}$ of 0.0003.

They also caused a considerable decrease in the aileron effectiveness $C_{l_{\delta_a}}$ and in $C_{h_{at}}$. At the higher angle of attack investigated ($\alpha = 9.0^\circ$) the roughness strips appeared to have a negligible effect on the aileron hinge moments but considerably reduced the aileron effectiveness in the large negative deflection range.

The location of the roughness strips was calculated to give approximately the same relative boundary-layer thickness at the aileron hinge line as would be found on the airplane in high speed flight where transition is expected to be at the leading edge of the wing. The airplane, therefore, would be expected to have greater aileron overbalance and less aileron effectiveness in high-speed flight than was found on the smooth model.

Effects of leakage.- The effects of various amounts of seal leakage on the aileron characteristics are shown in figures 17 to 19 and are summarized in figure 20. Figures 17 and 18 show that leakage not only reduces the effectiveness of the balance but also reduces the range of aileron deflections at which the balance is most effective. The largest amount of leakage investigated, however, did not reduce the balance effectiveness enough to eliminate the overbalance at low angles of attack.

The rolling-moment curves of figure 18 show that the leakage has its largest effect on the aileron effectiveness in the negative deflection range. Figure 20 and table II show that the range of leakage investigated caused a reduction in $C_{l_{\delta_a}}$ of approximately 17 percent and a reduction in $(\Delta P)_{\delta_a}$ of approximately 26 percent but had a negligible effect on $C_{h_{a\delta_t}}$.

CONCLUSIONS

An aileron investigation on a partial-span model of the Republic XF-12 airplane indicated the following conclusions:

1. The rate of change of aileron hinge-moment coefficient with aileron deflection had a positive value through a small range of aileron and tab deflections at low angles of attack with flaps neutral but as the angle of attack was increased or the flaps were deflected the rate of change decreased until at high angles of attack with flaps neutral or at moderate angles of attack with flaps deflected the rate of change became negative. This condition indicates the need for reducing the balancing effect to prevent illogical control wheel forces at high speeds.

2. At all flap deflections, the rate of change of aileron hinge-moment coefficient with angle of attack varied from positive values at low angles of attack to negative values at high angles of attack.

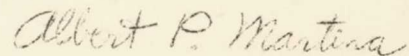
3. At conditions simulating high-speed flight, wing roughness tended to further increase the positive value of the rate of change of aileron hinge-moment coefficient with aileron deflection but reduced the rate of change of rolling-moment coefficient with aileron deflection.

4. Increasing the balance-seal leakage decreased the rate of change of both aileron hinge-moment coefficient and rolling-moment coefficient with aileron deflection but had a negligible effect on the rate of change of aileron hinge-moment coefficient with tab deflection.

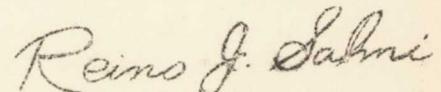
National Advisory Committee for Aeronautics
Langley Memorial Aeronautical Laboratory
Langley Field, Va.



Robert R. Graham
Aeronautical Engineer

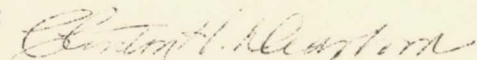


Albert P. Martina
Aeronautical Engineer



Reino J. Salmi
Aeronautical Engineer

Approved:



Clinton H. Dearborn
Chief of Full-Scale Research Division

BW

REFERENCES

- ✓ 1. Klein, Milton M.: Aerodynamic Characteristics of Four Republic Airfoil Sections from Tests in Langley Two-Dimensional Low-Turbulence Tunnels. NACA MR No. L5119, Army Air Forces, 1945.
- ✓ 2. Sivells, James C., and Deters, Owen J.: Jet-Boundary and Plan-Form Corrections for Partial-Span Models with Reflection Plane, End Plate, or No End Plate in a Closed Circular Wind Tunnel. NACA TN No. 1077, 1946.

TABLE I
 GEOMETRIC CONSTANTS OF REPUBLIC
 XF-12 AIRPLANE AND MODEL

	Full scale (6° dihedral)	1/4 scale (6° dihedral)	Partial-span model (0° dihedral)
S, sq ft	1640.	102.5	46.177
b, ft	129.167	32.292	15.006
c ² , ft	13.433	3.358	-----
b _a , ft	23.21	5.803	5.841
b _b , ft	20.67	5.168	5.550
c _a , ft	1.844	.461	.458
c _b , ft	.865	.216	.211
t, ft			.170
F			.170
F ₁			.098
F ₂			.072

NATIONAL ADVISORY
 COMMITTEE FOR AERONAUTICS

TABLE II

SUMMARY OF AILERON CHARACTERISTICS OF

$\frac{1}{4}$ -SCALE PARTIAL-SPAN MODEL OF XF-12 AIRPLANE

[All values measured over a small range of angles at $\delta_a = \delta_t = 0$]

Surface condition	α	δ_f	E	$C_{na\delta_a}$	$C_{na\alpha}$	$C_{na\delta_t}$	$C_{l\delta_a}$	$(\Delta P)_{\delta_a}$ (a)
Smooth	0.8	0	0.027	0.0016	0.0045	-0.0026	0.00160	0.064
Smooth	4.7			.0004	.0011	-.0030	.00155	.054
Smooth	9.0			-.0034	-.0027	-.0029	.00134	.039
Smooth	13.6			-.0047	-.0056	-.0029	.00127	.038
Smooth	.8		.072	.0009	-----	-.0027	.00146	.058
Smooth	9.0			-.0042	-----	-.0027	.00115	.036
Smooth	.8		.116	.0006	-----	-----	.00138	.048
Smooth	9.0			-.0048	-----	-----	.00119	.025
Roughness strips at 0.20c	.8		.027	.0019	-----	.0021	.00130	.048
Roughness strips at 0.20c	9.0			-.0033	-----	-----	.00132	.037
Smooth	3.2	20		.0002	.0017	-.0031	.00165	.071
Smooth	8.4			-.0034	-.0031	-.0030	.00145	.052
Smooth	14.3			-.0052	-.0055	-.0026	.00110	.043
Smooth	-3.0	55		.0003	.0021	-.0031	.00173	.078
Smooth	2.3			-.0016	.0010	-.0031	.00165	.071
Smooth	7.4			-.0052	-.0031	-.0031	.00162	.059
Smooth	12.1			-.0070	-.0046	-.0032	.00145	.052

^a Inboard chamber.

FIGURE LEGENDS

Figure 1.- Three-view drawing of the Republic XF-12 airplane.

Figure 2.- Plan and elevation of the $\frac{1}{4}$ -scale partial-span model of the XF-12 airplane wing.

Figure 3.- Arrangement of the $\frac{1}{4}$ -scale XF-12 partial-span model and reflection plane in the Langley 19-foot pressure tunnel.

Figure 4.- $\frac{1}{4}$ -scale partial-span model of the XF-12 airplane mounted in the 19-foot pressure tunnel.

(a) Front view.

Figure 4.- Concluded.

(b) rear view.

Figure 5.- Plan view and typical cross section of aileron and tab; $\frac{1}{4}$ -scale partial-span model of the XF-12 airplane.

Figure 6.- Variation of vent gap along span of aileron.

Figure 7.- Typical section of double-slotted flaps on the $\frac{1}{4}$ -scale partial-span model of the Republic XF-12 airplane.

Figure 8.- Effect of holes in aileron balance nose on seal leakage factor.

Figure 9.- Aileron and tab characteristics of $\frac{1}{4}$ -scale partial-span model of the XF-12 airplane. Smooth model; $\delta_f = 0^\circ$; $E = 0.027$.

(a) $\alpha = 0.8^\circ$.

Figure 9.- Continued.

(b) $\alpha = 4.7^\circ$.

Figure 9.- Continued.

(c) $\alpha = 9.0^\circ$.

Figure 9.- Concluded.

(d) $\alpha = 13.6^\circ$.

FIGURE LEGENDS - Continued

Figure 10.- Aileron and tab characteristics of $\frac{1}{4}$ -scale partial-span model of the XF-12 airplane. Smooth model; $\delta_F = 20^\circ$; $E = 0.027$.

(a) $\alpha = 3.2^\circ$.

Figure 10.- Continued.

(b) $\alpha = 8.4^\circ$.

Figure 10.- Concluded.

(c) $\alpha = 14.3^\circ$.

Figure 11.- Aileron and tab characteristics of $\frac{1}{4}$ -scale partial-span model of the XF-12 airplane. Smooth model; $\frac{1}{4}\delta_F = 55^\circ$; $E = 0.027$.

(a) $\alpha = -3.0^\circ$.

Figure 11.- Continued.

(b) $\alpha = 2.3^\circ$.

Figure 11.- Continued.

(c) $\alpha = 7.4^\circ$.

Figure 11.- Concluded.

(d) $\alpha = 12.1^\circ$.

Figure 12.- Pressure coefficients across aileron balance on $\frac{1}{4}$ -scale partial-span model of the XF-12 airplane. Smooth model; $\delta_t = 0^\circ$; $E = 0.027$.

(a) $\delta_F = 0^\circ$.

Figure 12.- Continued.

(b) $\delta_F = 20^\circ$.

Figure 12.- Concluded.

(c) $\delta_F = 55^\circ$.

FIGURE LEGENDS - Continued

Figure 13.- Variation of aileron hinge-moment coefficient with angle of attack on the $\frac{1}{4}$ -scale partial-span model of the XF-12 airplane.

Smooth model; $\delta_a = 0^\circ$; $\delta_t = 0^\circ$; $E = 0.027$.

Figure 14.- Aileron and tab characteristics of $\frac{1}{4}$ -scale partial-span

model of the XF-12 airplane. Roughness strips at $0.20c$; $\delta_f = 0^\circ$; $\alpha = 0.8^\circ$; $E = 0.027$.

Figure 15.- Effects of roughness strips at $0.20c$ on aileron

characteristics of $\frac{1}{4}$ -scale partial-span model of the XF-12 airplane.

$\delta_f = 0^\circ$; $\delta_t = 0^\circ$; $E = 0.027$.

Figure 16.- Pressure coefficients across aileron balance on $\frac{1}{4}$ -scale

partial-span model of the XF-12 airplane. Roughness strips at $0.20c$; $\delta_f = 0^\circ$; $\delta_t = 0^\circ$; $E = 0.027$.

Figure 17.- Aileron and tab characteristics of $\frac{1}{4}$ -scale partial-span

model of the XF-12 airplane. Smooth model; $\delta_f = 0^\circ$; $E = 0.072$.

(a) $\alpha = 0.8^\circ$.

Figure 17.- Concluded.

(b) $\alpha = 9.0^\circ$.

Figure 18.- Effects of various amounts of leakage on the aileron

characteristics of $\frac{1}{4}$ -scale partial-span model of the XF-12 airplane.

Smooth model; $\delta_f = 0^\circ$; $\delta_t = 0^\circ$.

(a) $\alpha = 0.8^\circ$.

Figure 18.- Concluded.

(b) $\alpha = 9.0^\circ$.

Figure 19.- Effects of various amounts of leakage on the pressure

coefficients across the aileron balance of $\frac{1}{4}$ -scale partial-span

model of the XF-12 airplane. Smooth model; $\delta_f = 0^\circ$; $\delta_t = 0^\circ$.

(a) $\alpha = 0.8^\circ$.

FIGURE LEGENDS - Concluded

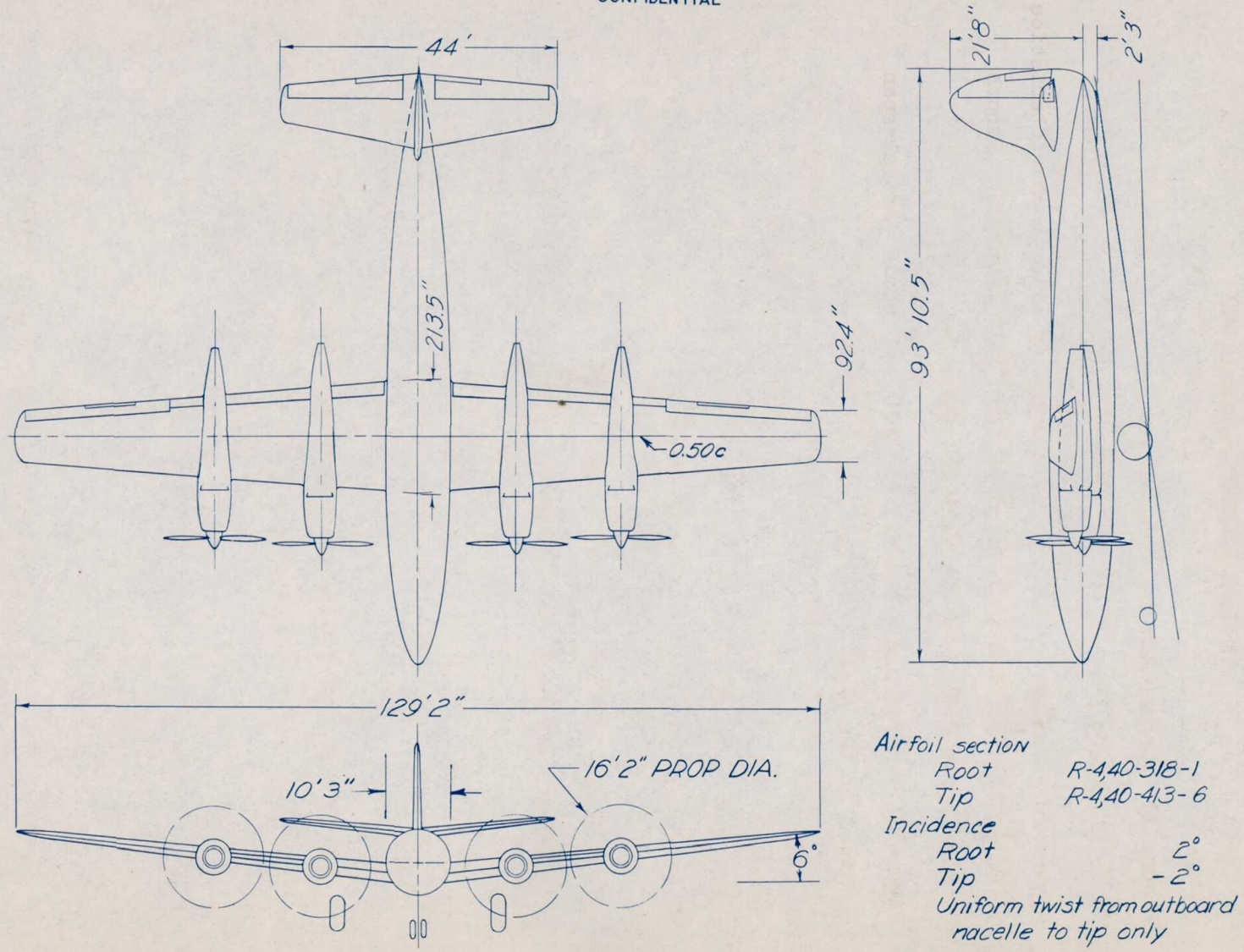
Figure 19.- Concluded.

(b) $\alpha = 9.0^\circ$.

Figure 20.- Summary of effects of leakage on aileron characteristics of $\frac{1}{4}$ -scale partial-span model of the XF-12 airplane. Smooth model; $\alpha = 0.8^\circ$; $\delta_a = 0^\circ$; $\delta_f = 0^\circ$; $\delta_t = 0^\circ$.

Figure 21.- Aerodynamic characteristics of $\frac{1}{4}$ -scale partial-span model of the XF-12 airplane. $\delta_a = 0^\circ$; $\delta_t = 0^\circ$.

CONFIDENTIAL



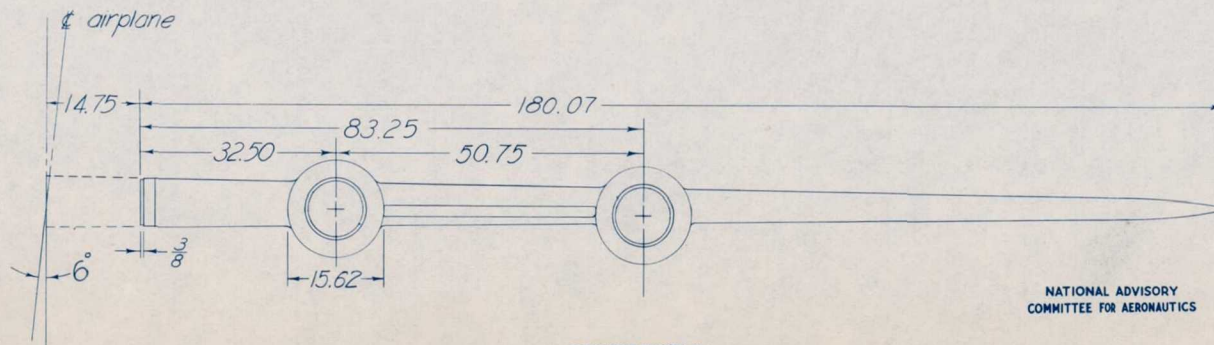
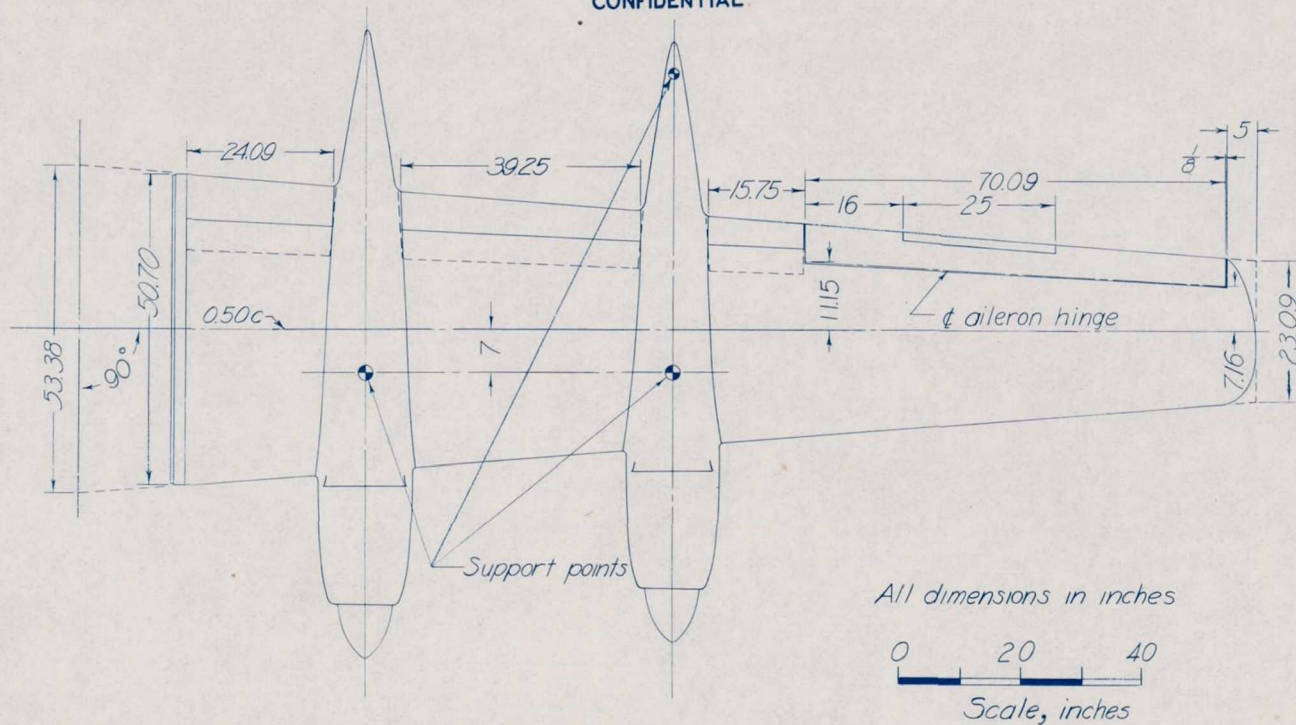
NATIONAL ADVISORY
 COMMITTEE FOR AERONAUTICS

NACA RM No. L6118

CONFIDENTIAL

Figure 1.- Three-view drawing of the Republic XF-12 airplane.

CONFIDENTIAL

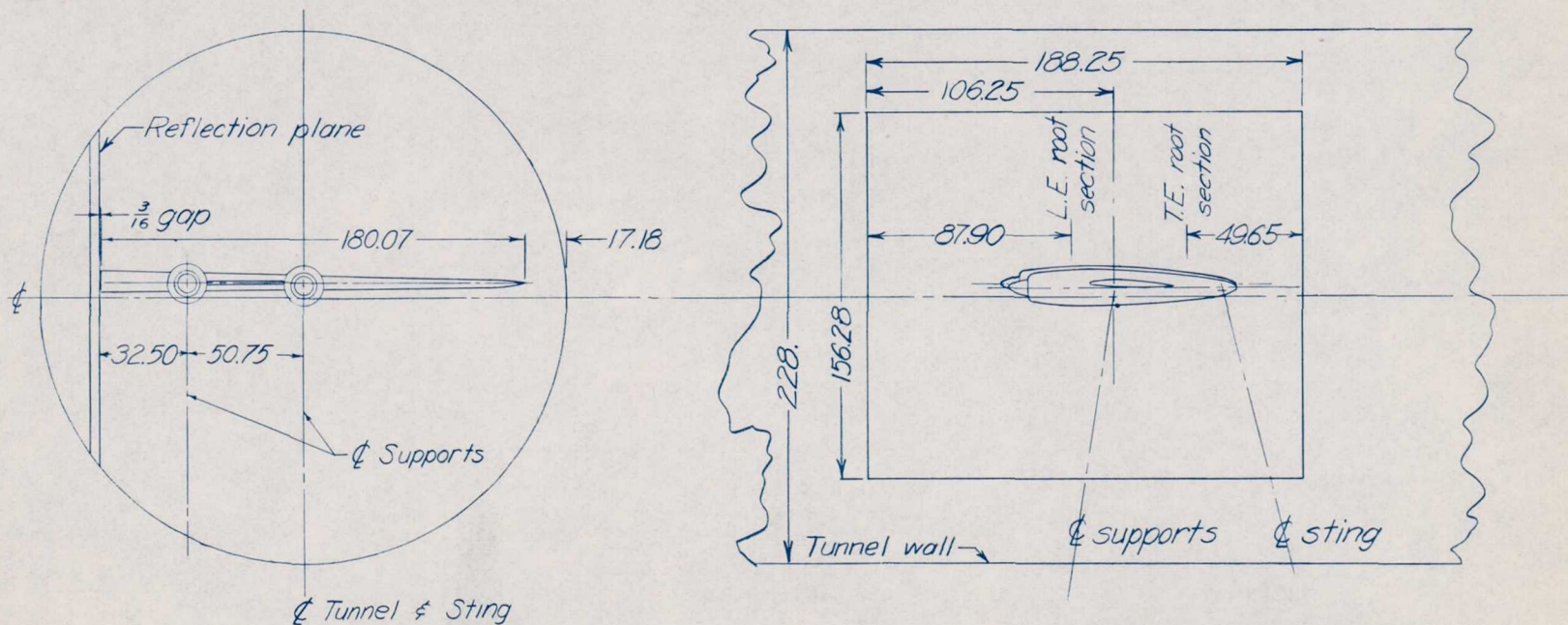


NATIONAL ADVISORY
COMMITTEE FOR AERONAUTICS

CONFIDENTIAL

Figure 2.- Plan and elevation of the $\frac{1}{4}$ -scale partial-span model of the XF-12 airplane wing

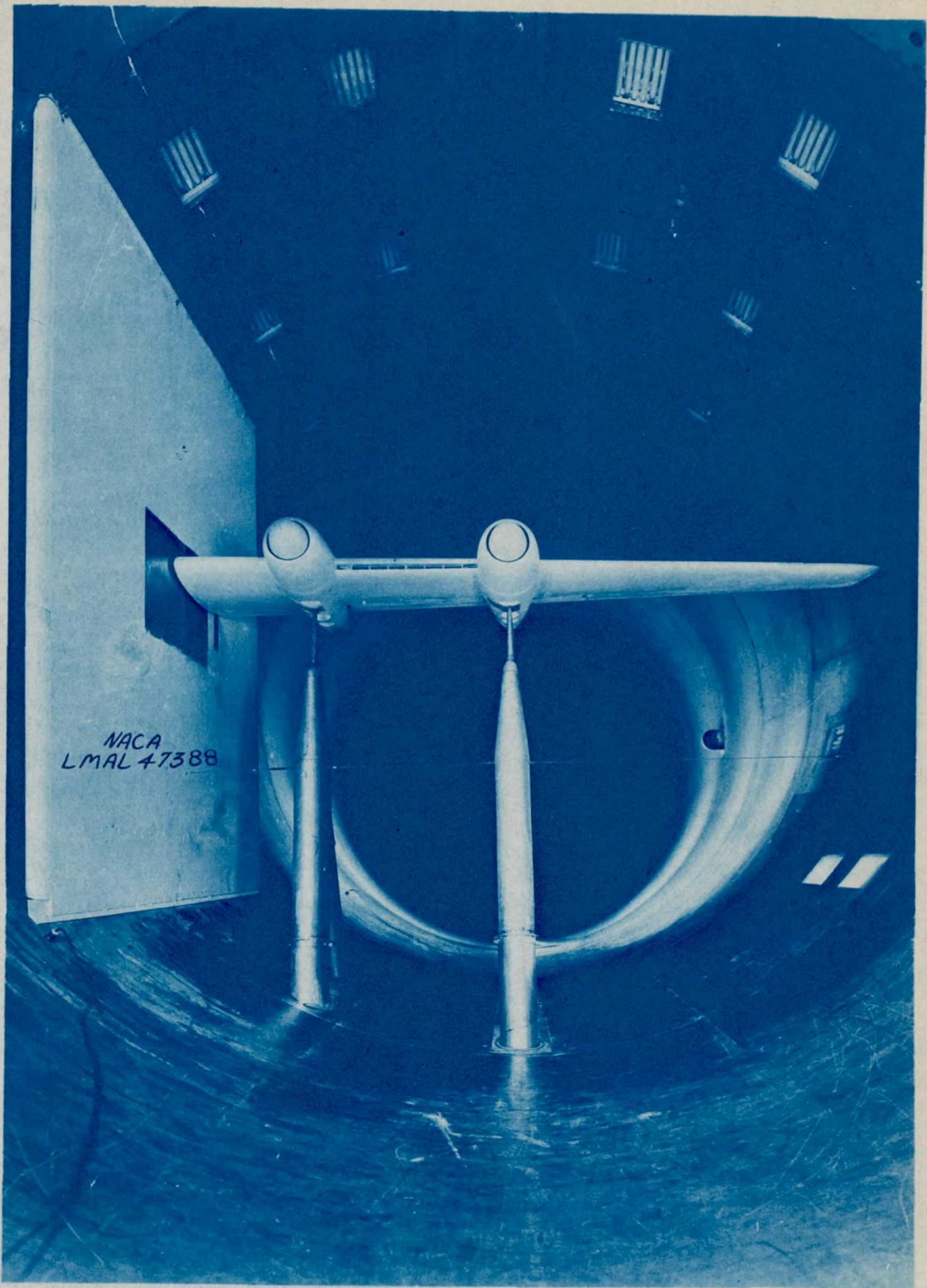
CONFIDENTIAL



CONFIDENTIAL

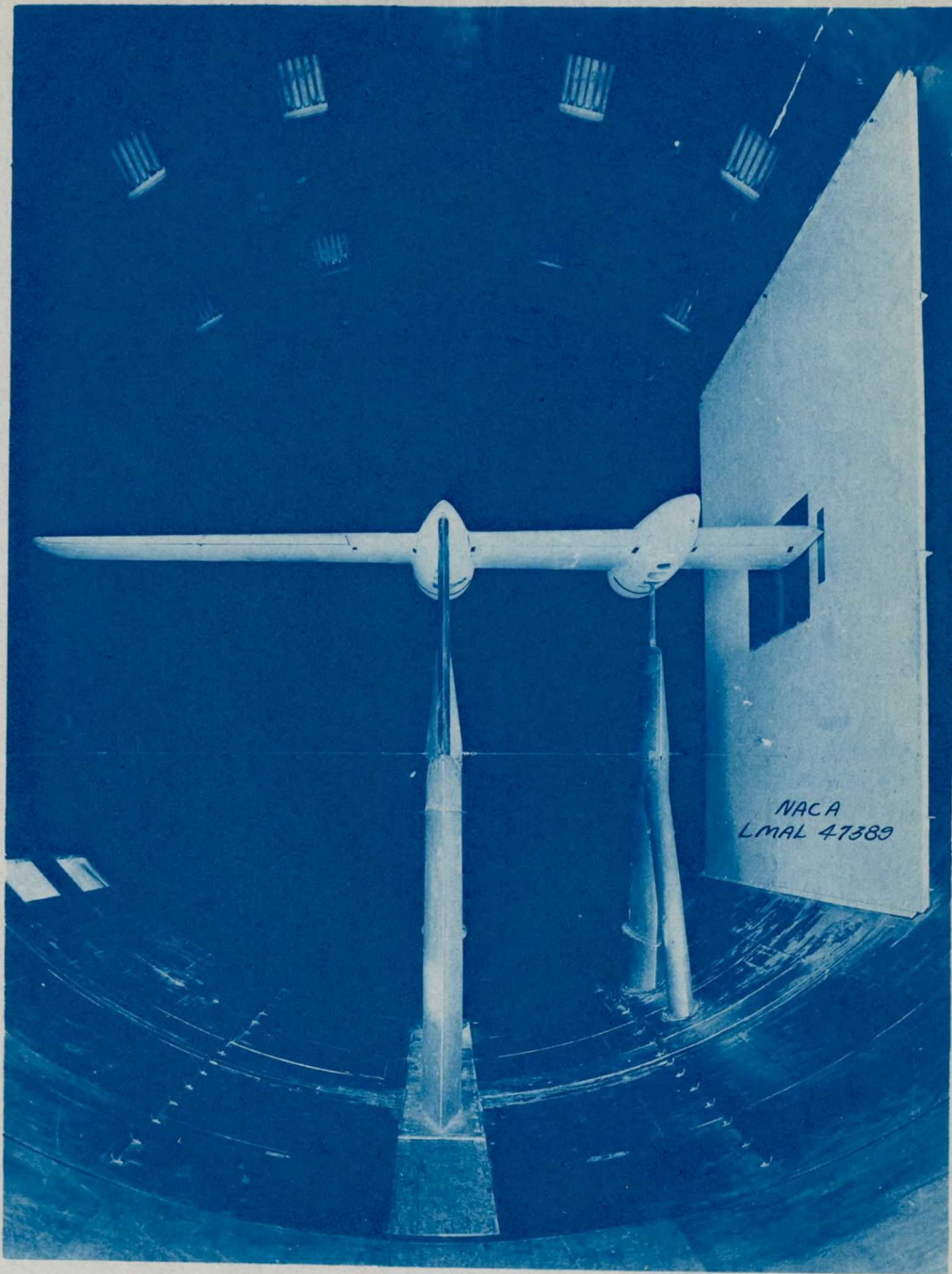
NATIONAL ADVISORY
COMMITTEE FOR AERONAUTICS

Figure 3.-Arrangement of the 1/4-scale XF-12 partial-span model and reflection plane in the Langley 19-foot pressure tunnel.



(a) Front view. **CONFIDENTIAL**

Figure 4.- $\frac{1}{4}$ -scale partial-span model of the XF-12 airplane mounted in the 19-foot pressure tunnel.

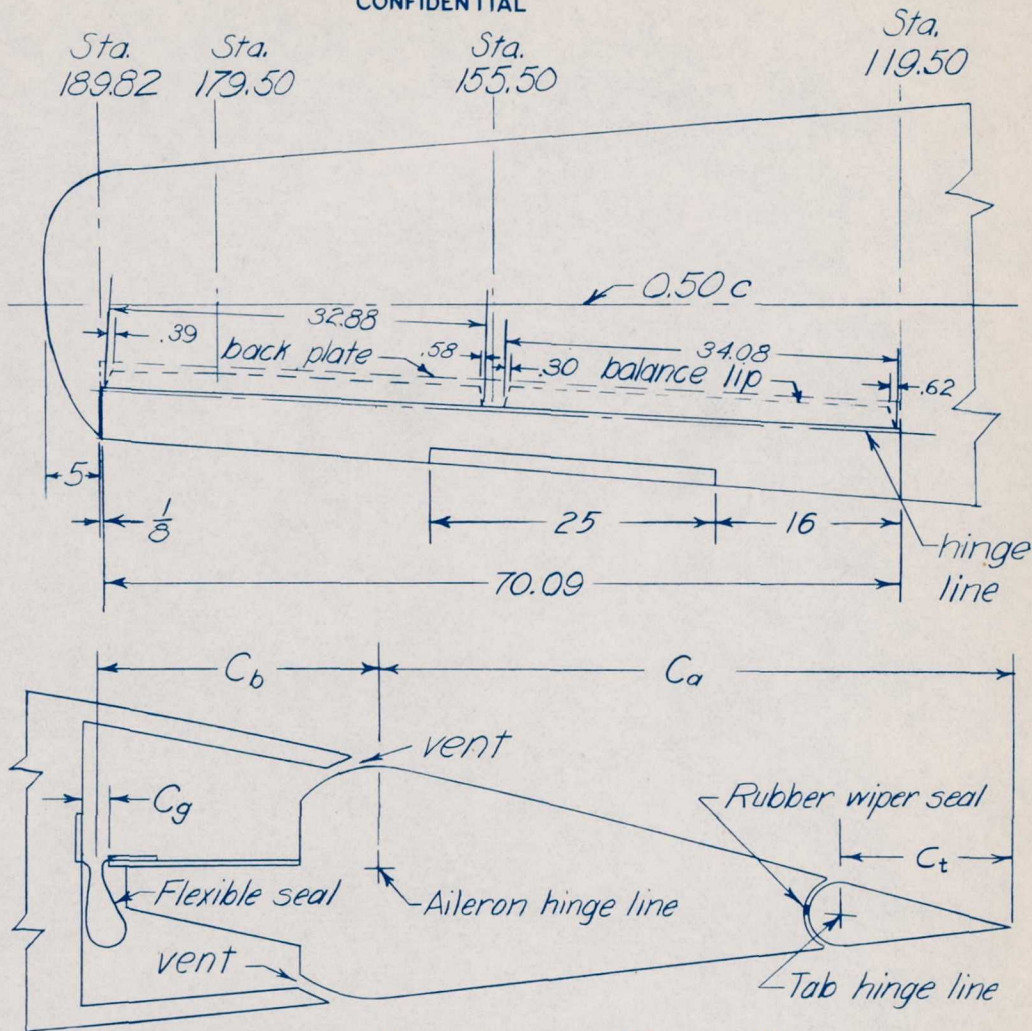


(b) Rear view.

CONFIDENTIAL

Figure 4.- Concluded.

CONFIDENTIAL



For dimensions of vents see Figure 6.

All dimensions in inches.

NATIONAL ADVISORY
COMMITTEE FOR AERONAUTICS

Station ^(a)	c	C_a	C_b	C_g	C_t	s ^(b)
119.50	34.81	6.26	2.93	0.25	-	1.27
155.50	29.20	5.49	2.55	0.28	1.50	1.26
179.50	25.47	5.00	2.30	0.34	-	1.59
189.82	23.88	4.78	2.07	0.56	-	1.23

^(a)Distance from fuselage centerline. ^(b)Developed seal width.

Figure 5. - Plan view and typical cross section of aileron and tab; $\frac{1}{4}$ -scale partial-span model of the XF-12 airplane.

CONFIDENTIAL

CONFIDENTIAL

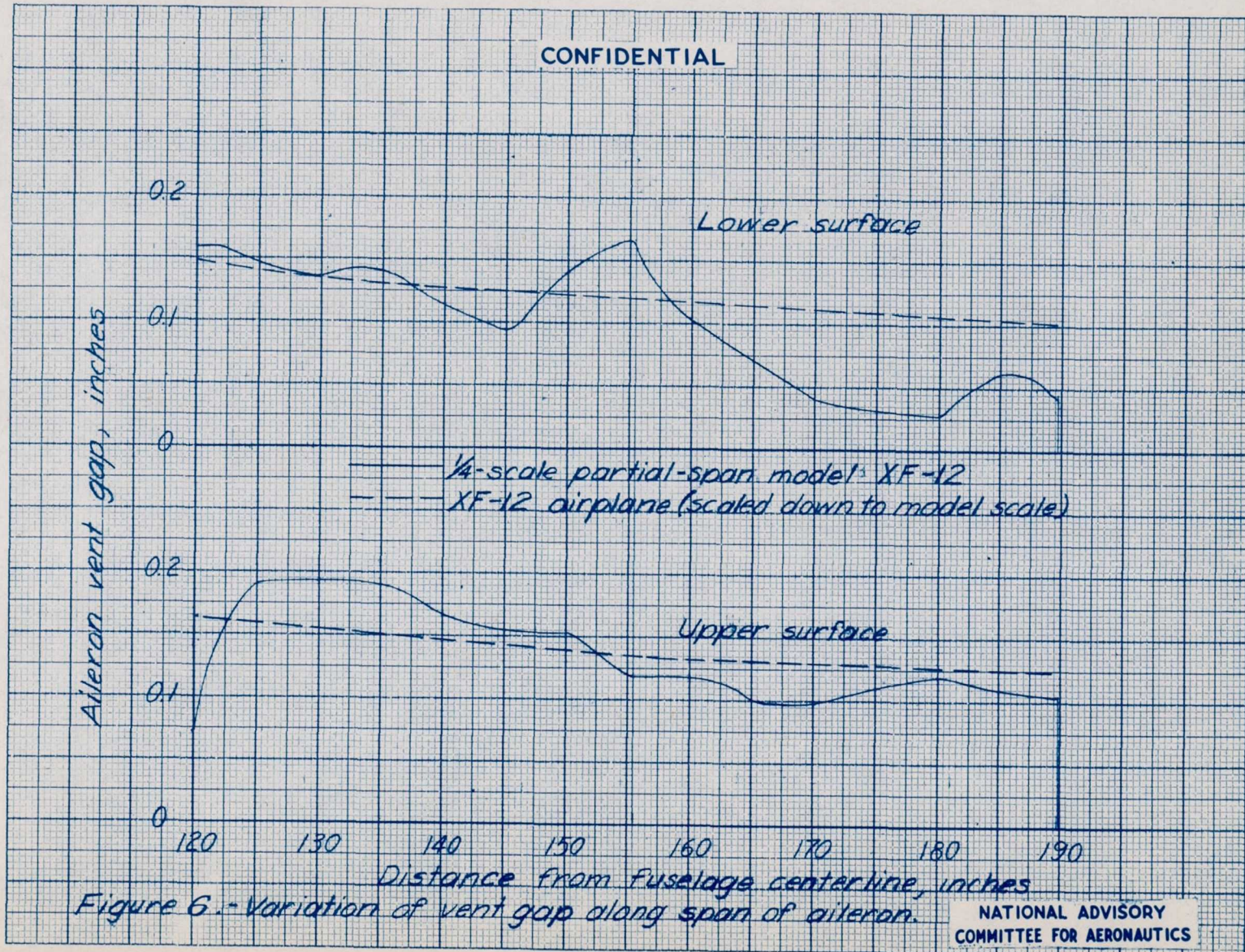
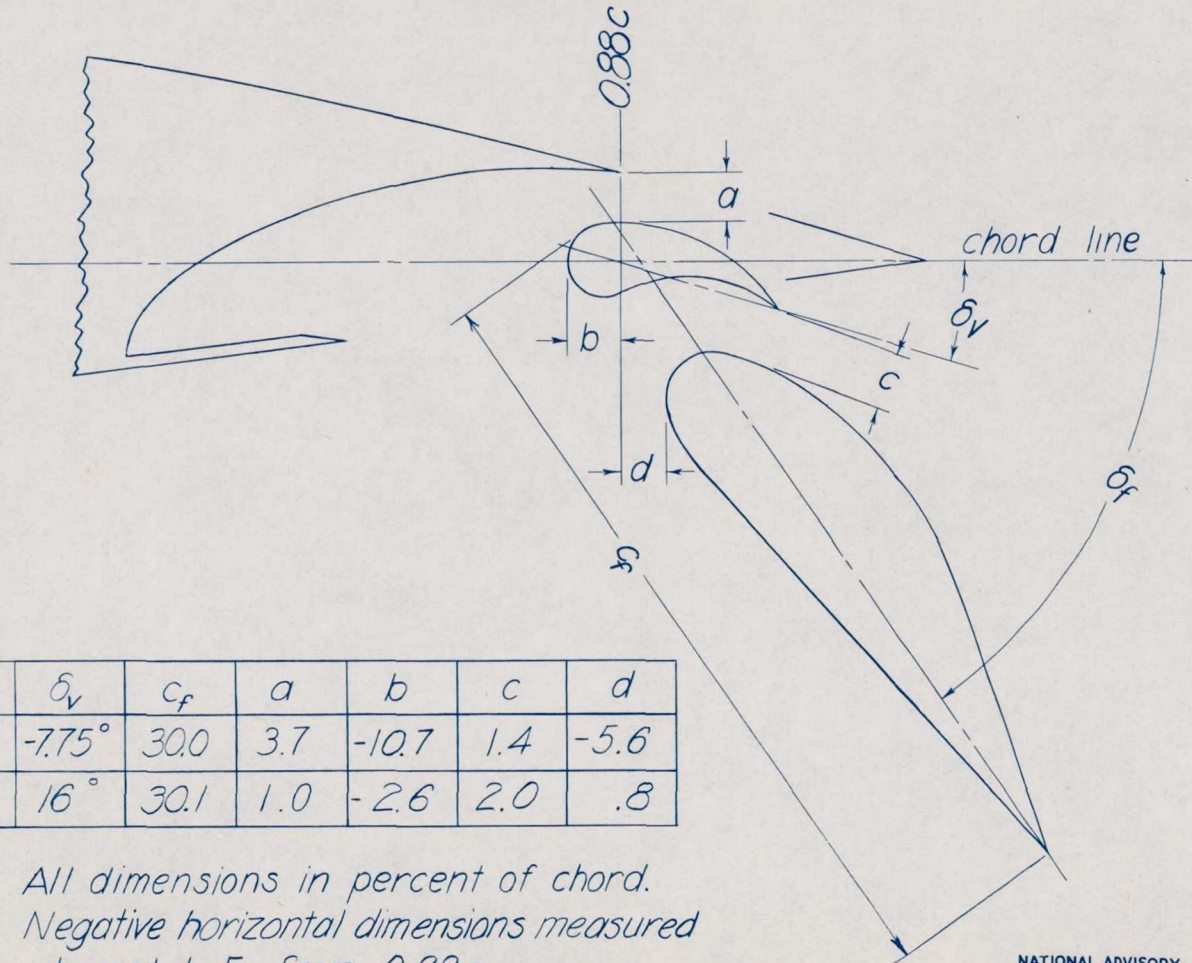


Figure 6 - Variation of vent gap along span of aileron.

NATIONAL ADVISORY
COMMITTEE FOR AERONAUTICS

CONFIDENTIAL

CONFIDENTIAL



δ_f	δ_v	c_f	a	b	c	d
20°	-7.75°	30.0	3.7	-10.7	1.4	-5.6
55°	16°	30.1	1.0	-2.6	2.0	.8

All dimensions in percent of chord.
 Negative horizontal dimensions measured
 toward L.E. from 0.88c.

NATIONAL ADVISORY
 COMMITTEE FOR AERONAUTICS

CONFIDENTIAL

Figure 7.- Typical section of double-slotted flaps on the $1/4$ -scale partial-span model of the Republic XF-12 airplane.

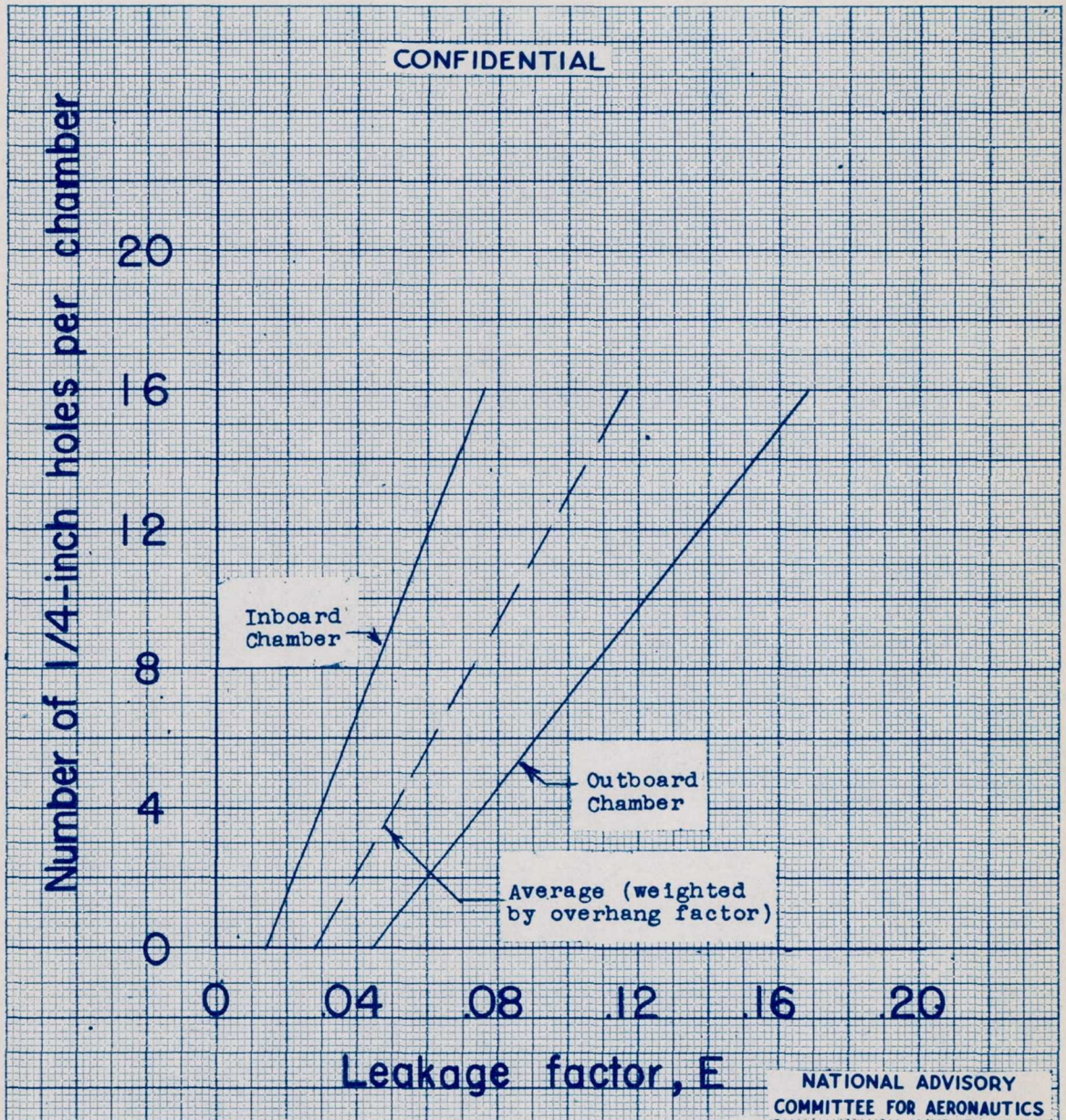
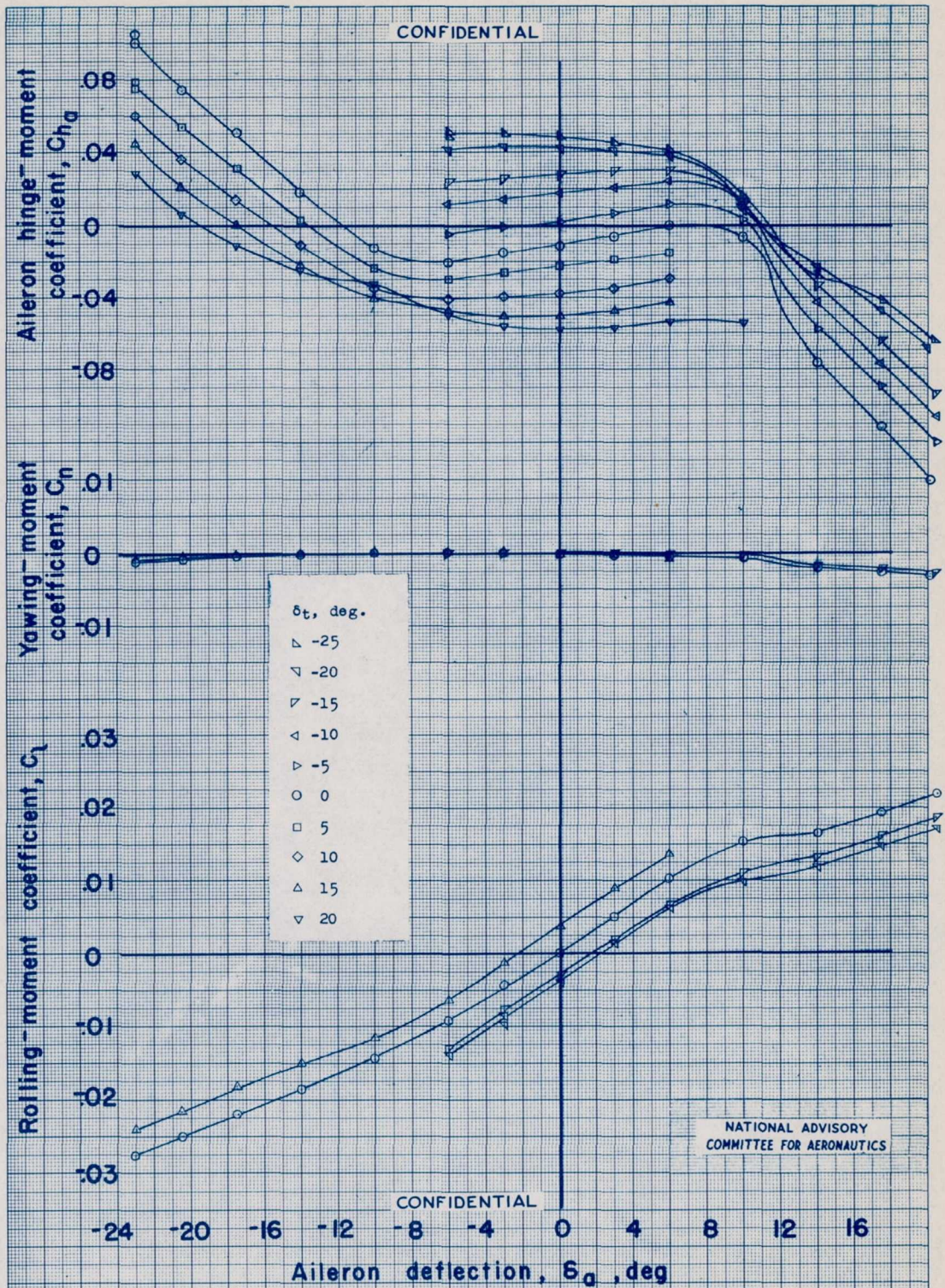
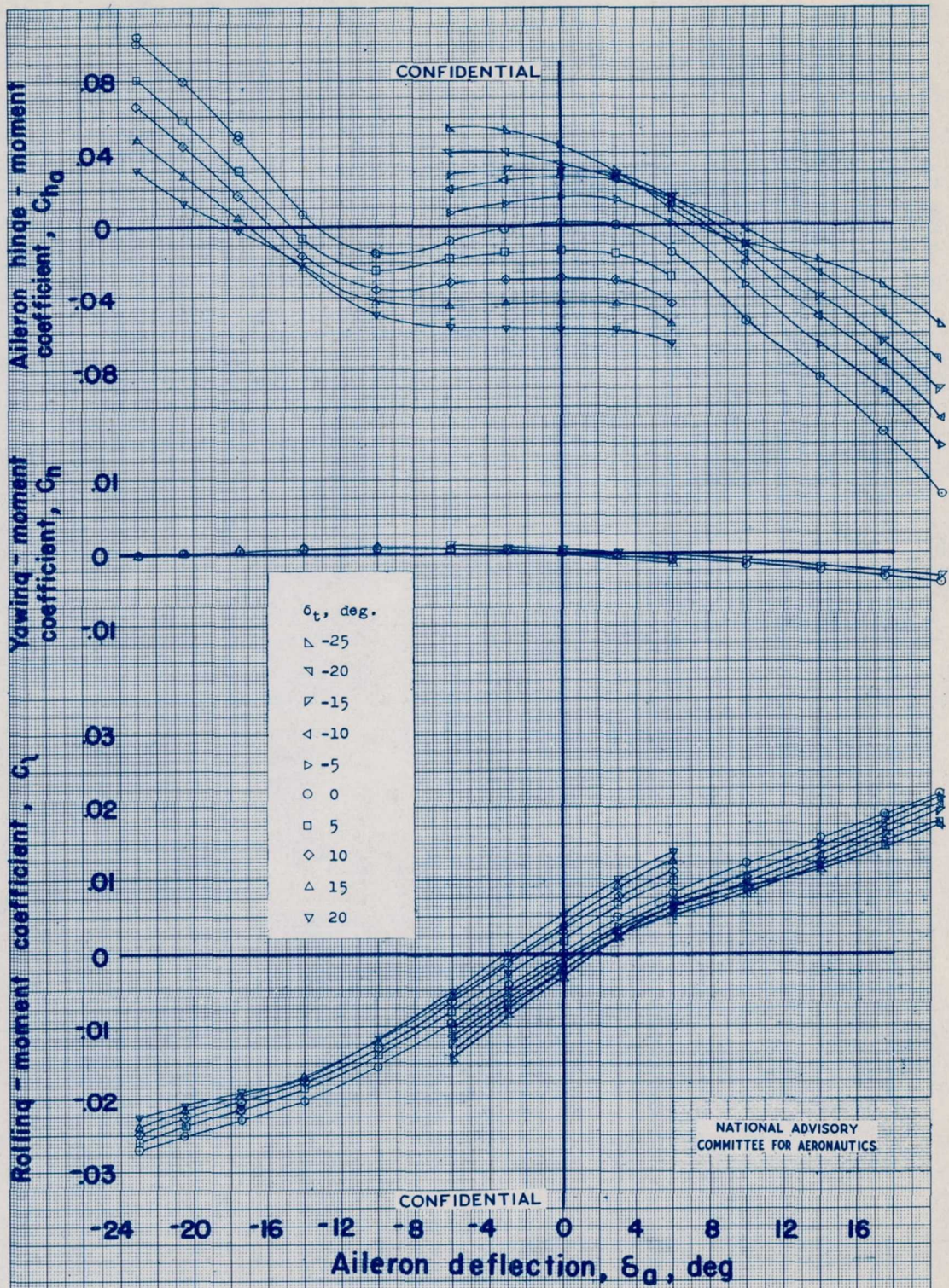


Figure 8. - Effect of holes in aileron balance nose on seal leakage factor.



(a) $\alpha = 0.8^\circ$

Figure 9.- Aileron and tab characteristics of 1/4-scale partial-span model of the XP-12 airplane. Smooth model; $\delta_f = 0^\circ$; $E = 0.027$.



(b) $\alpha = 4.7^\circ$

Figure 9.- Continued.

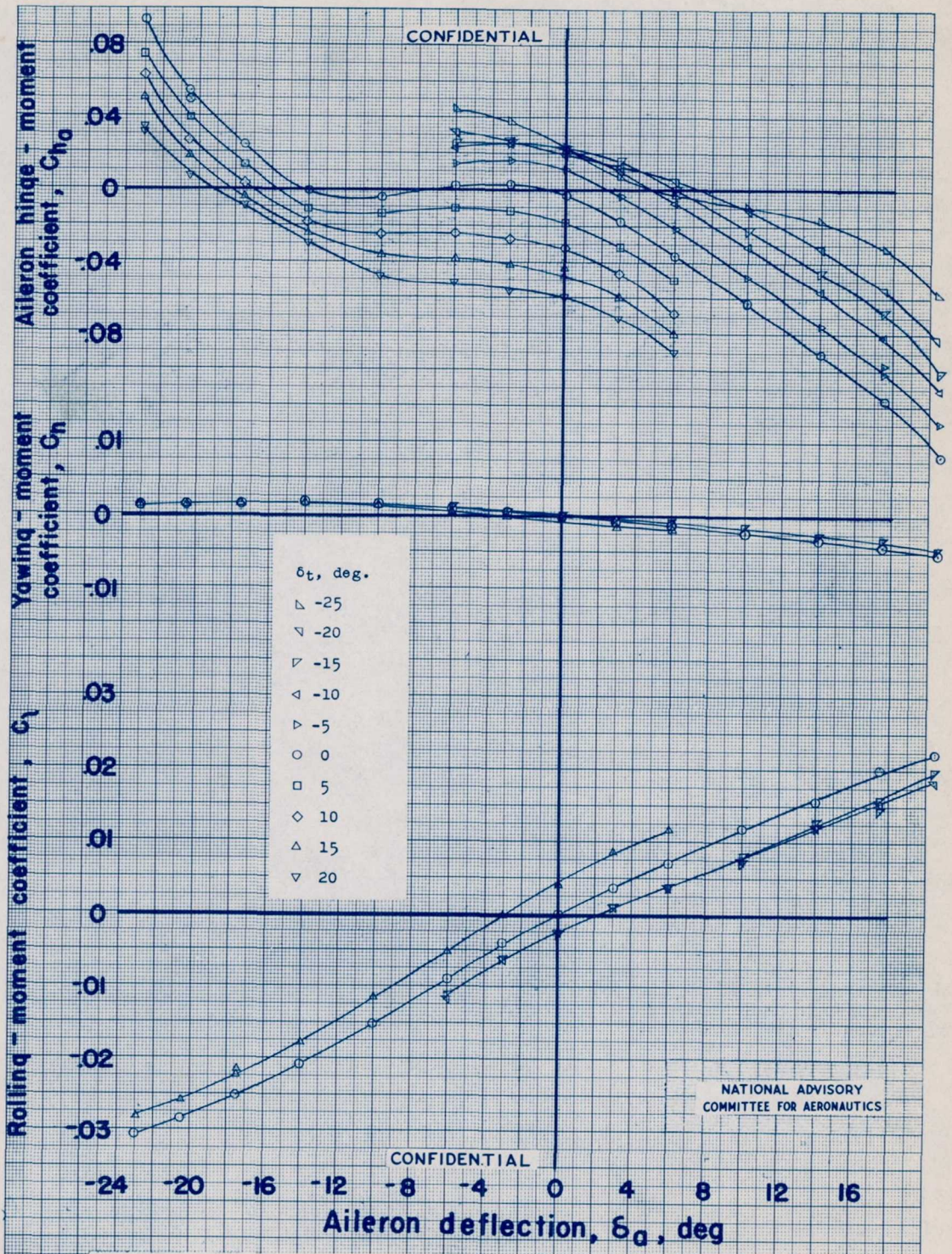
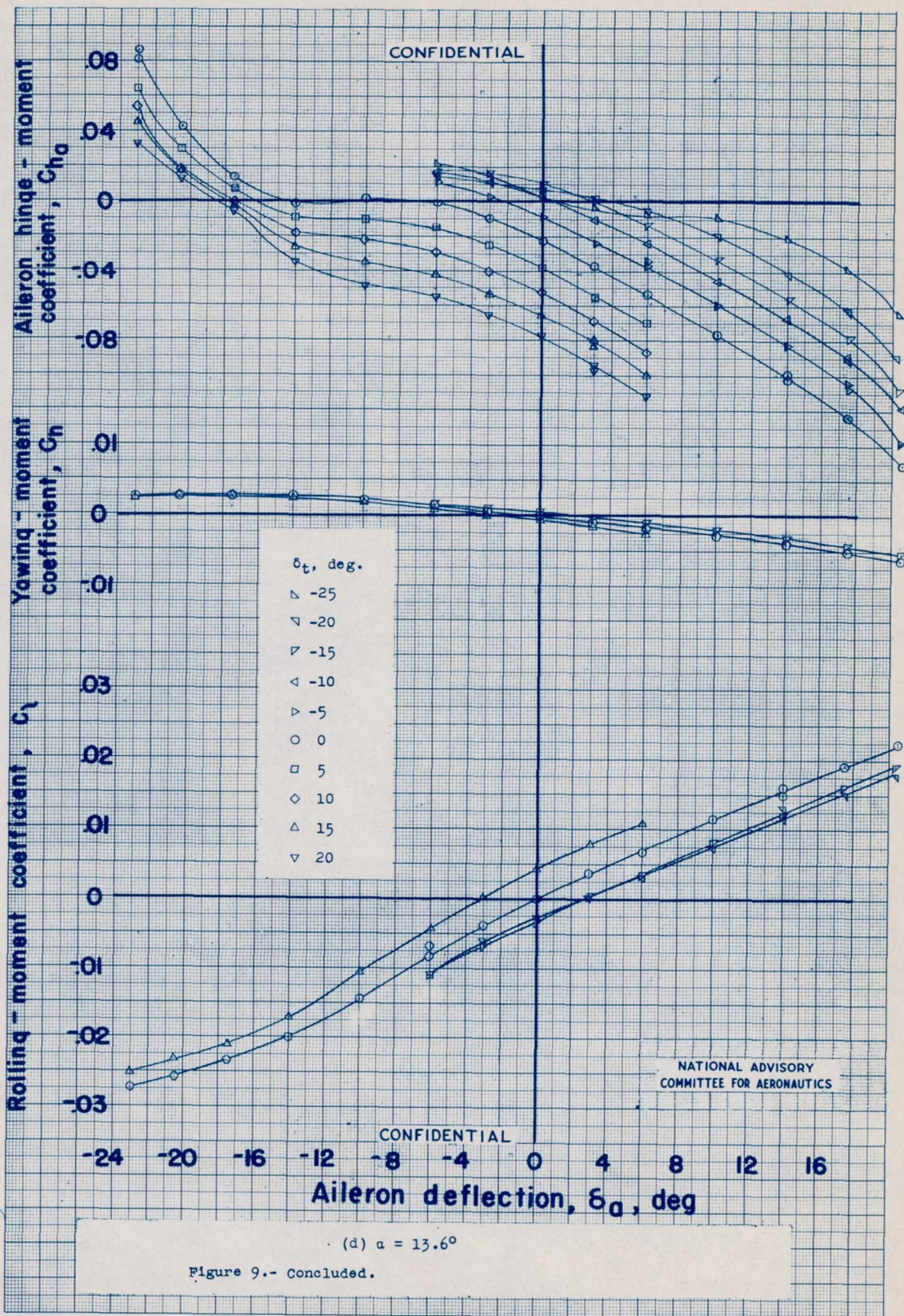
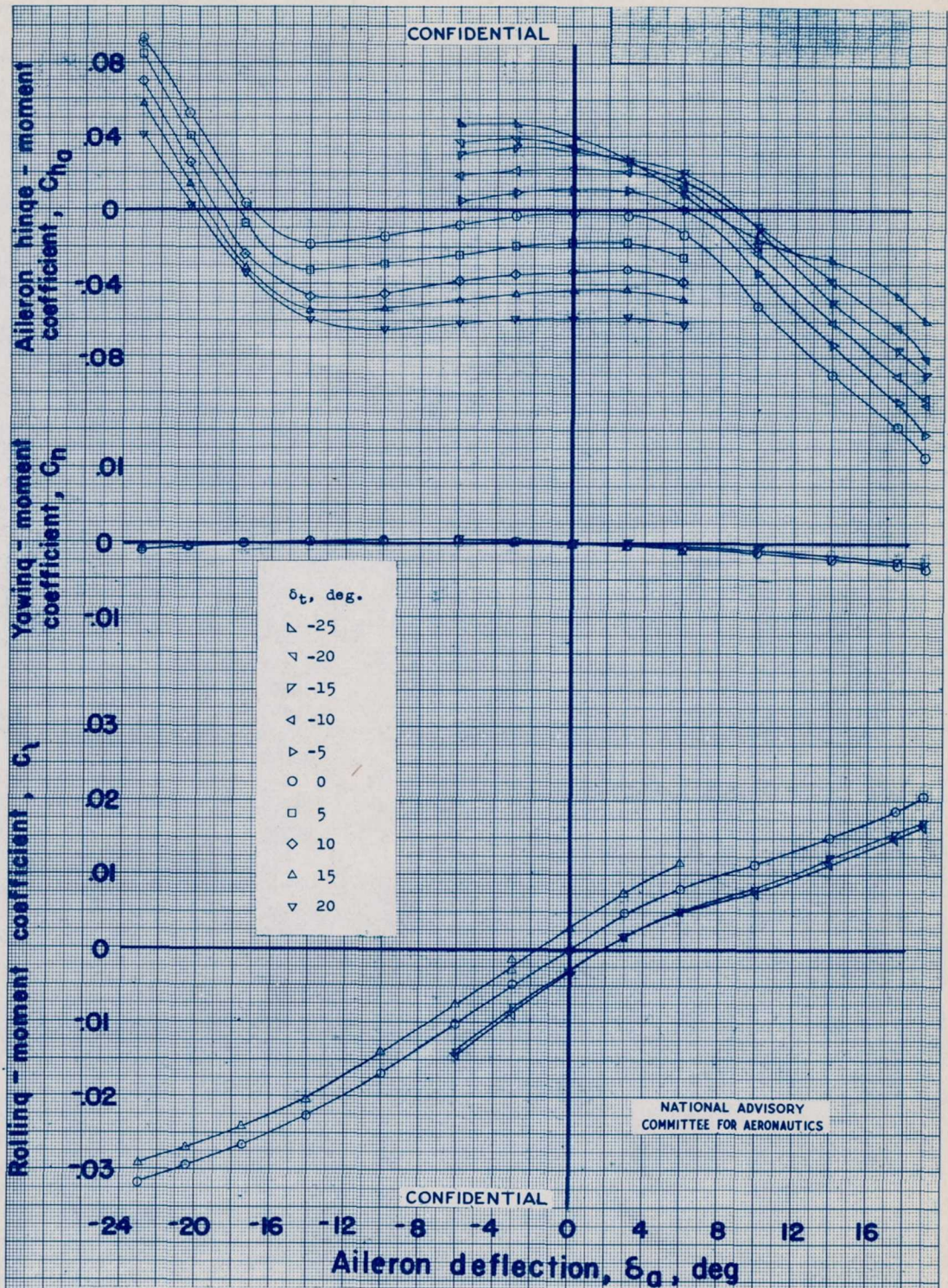


Figure 9.- Continued.





(a) $\alpha = 3.2^\circ$

Figure 10.- Aileron and tab characteristics of 1/4-scale partial-span model of the XF-12 airplane. Smooth model; $\delta_r = 20^\circ$; $E = 0.027$.

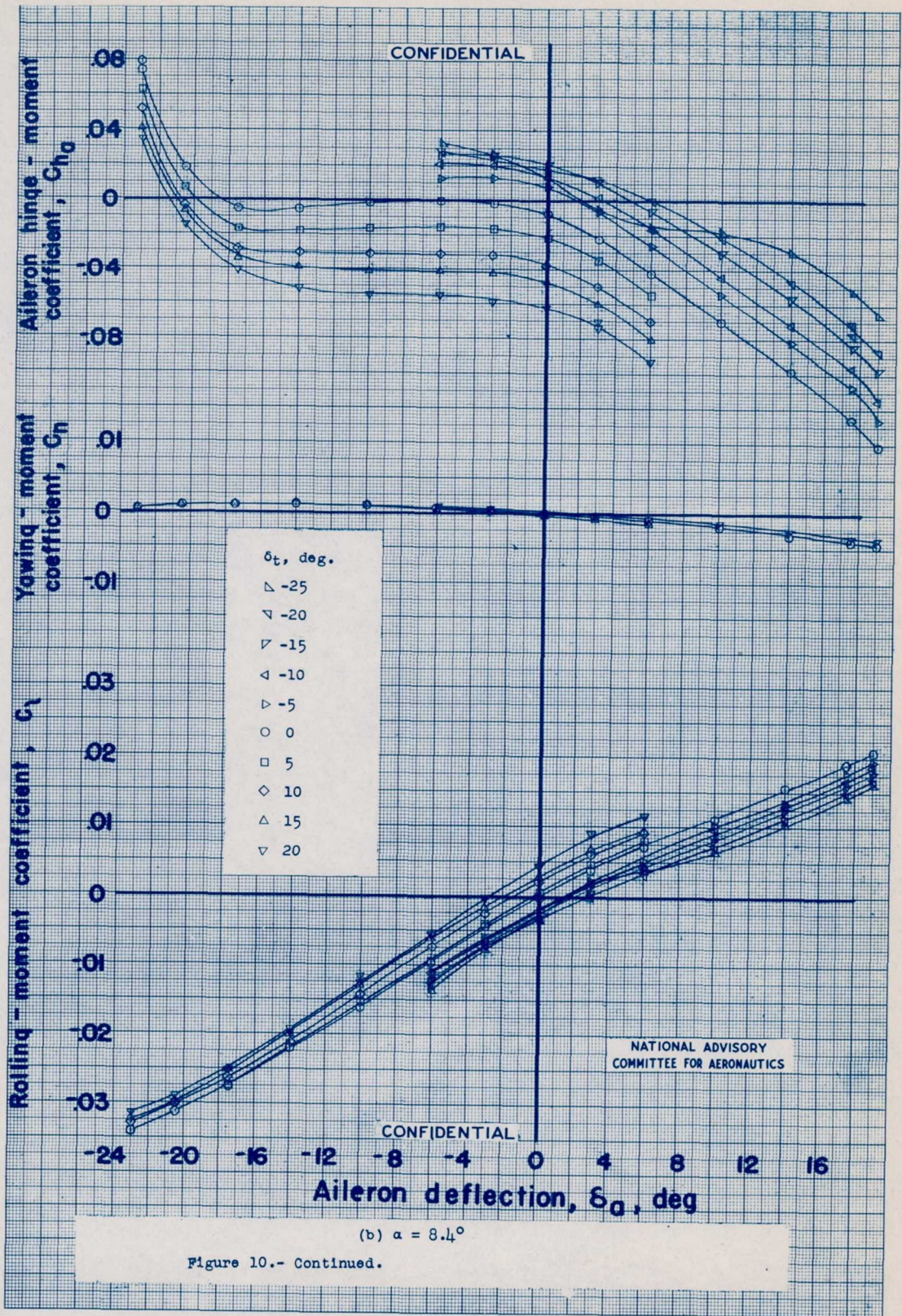


Figure 10.- Continued.

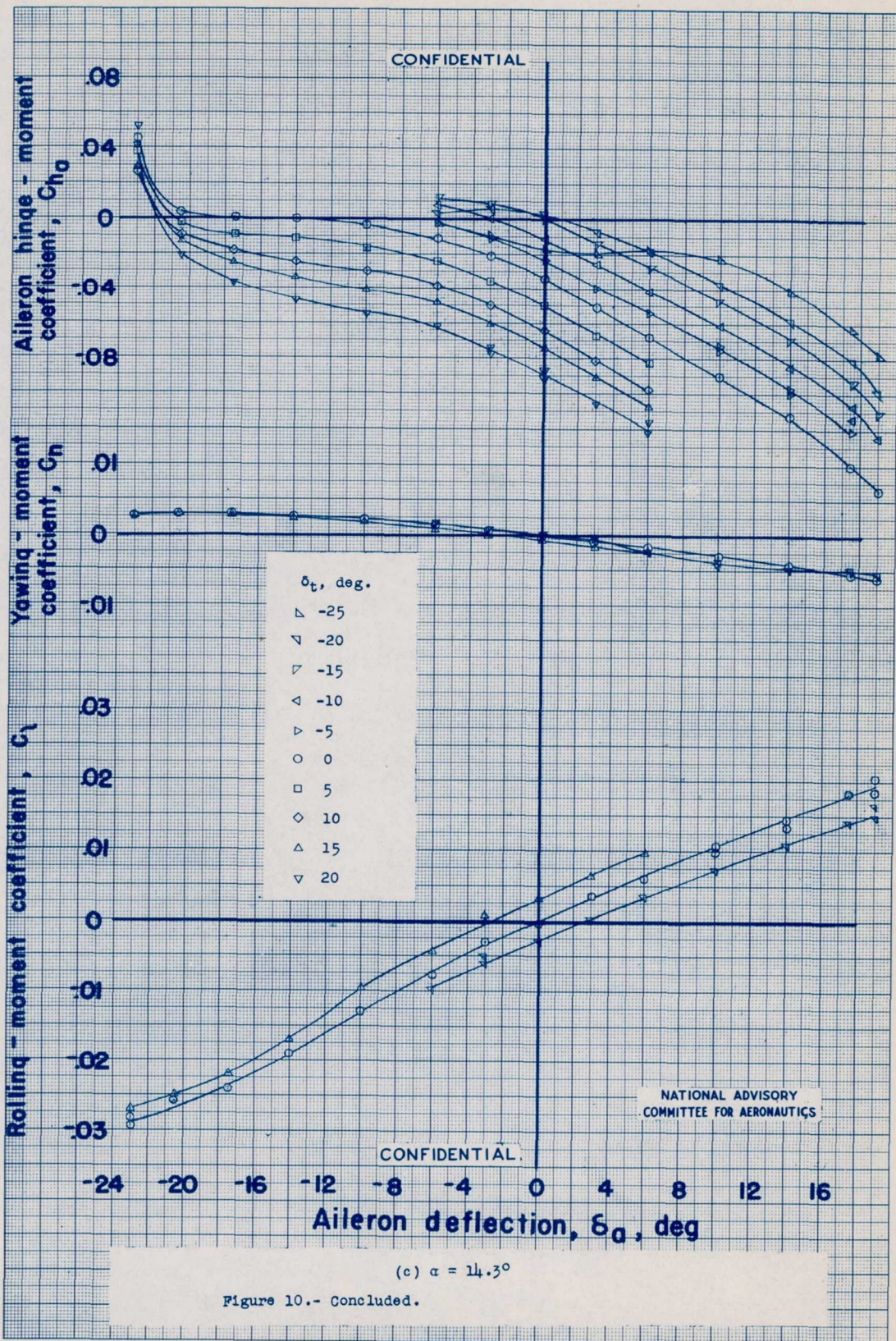


Figure 10.- Concluded.

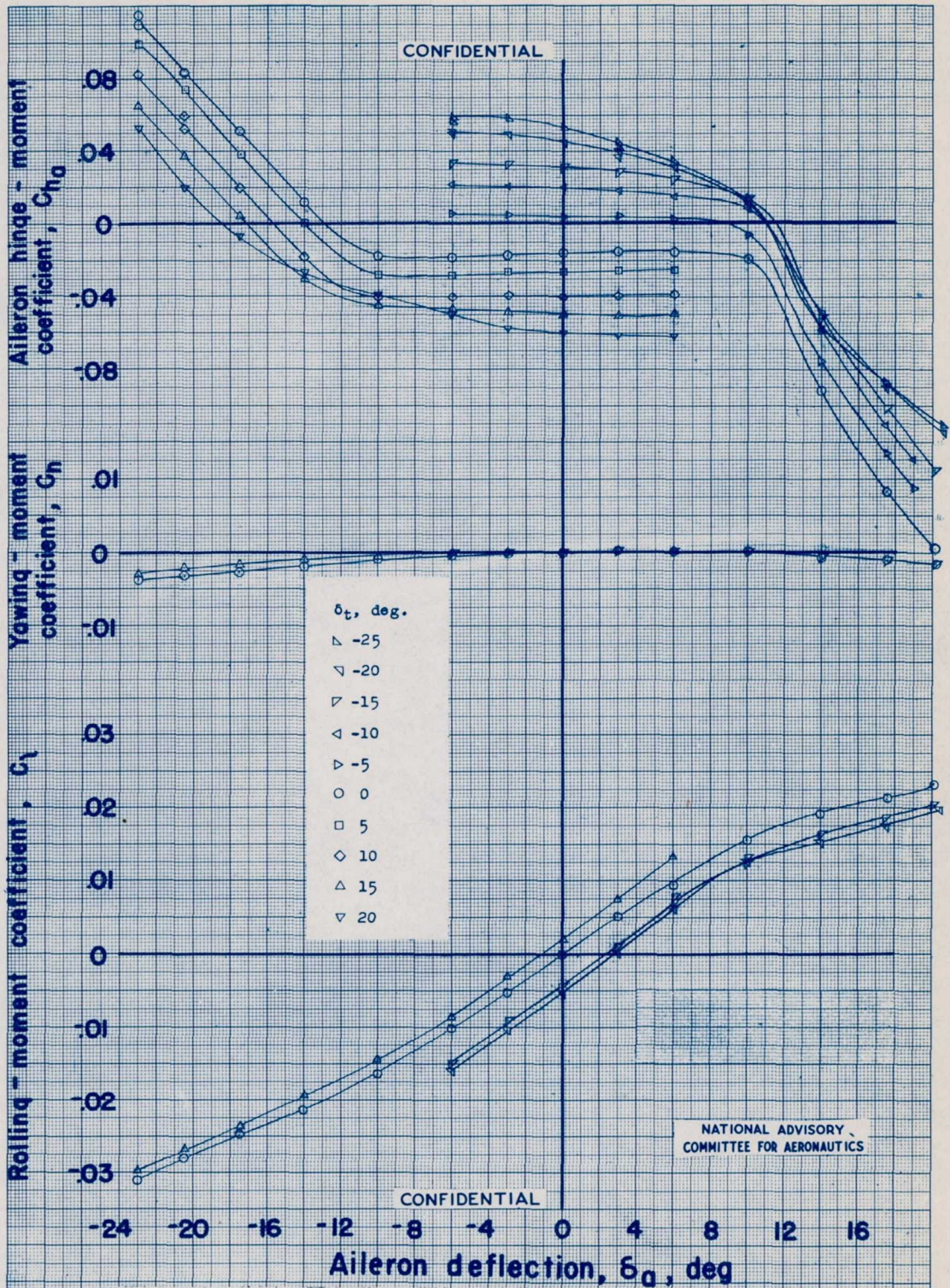
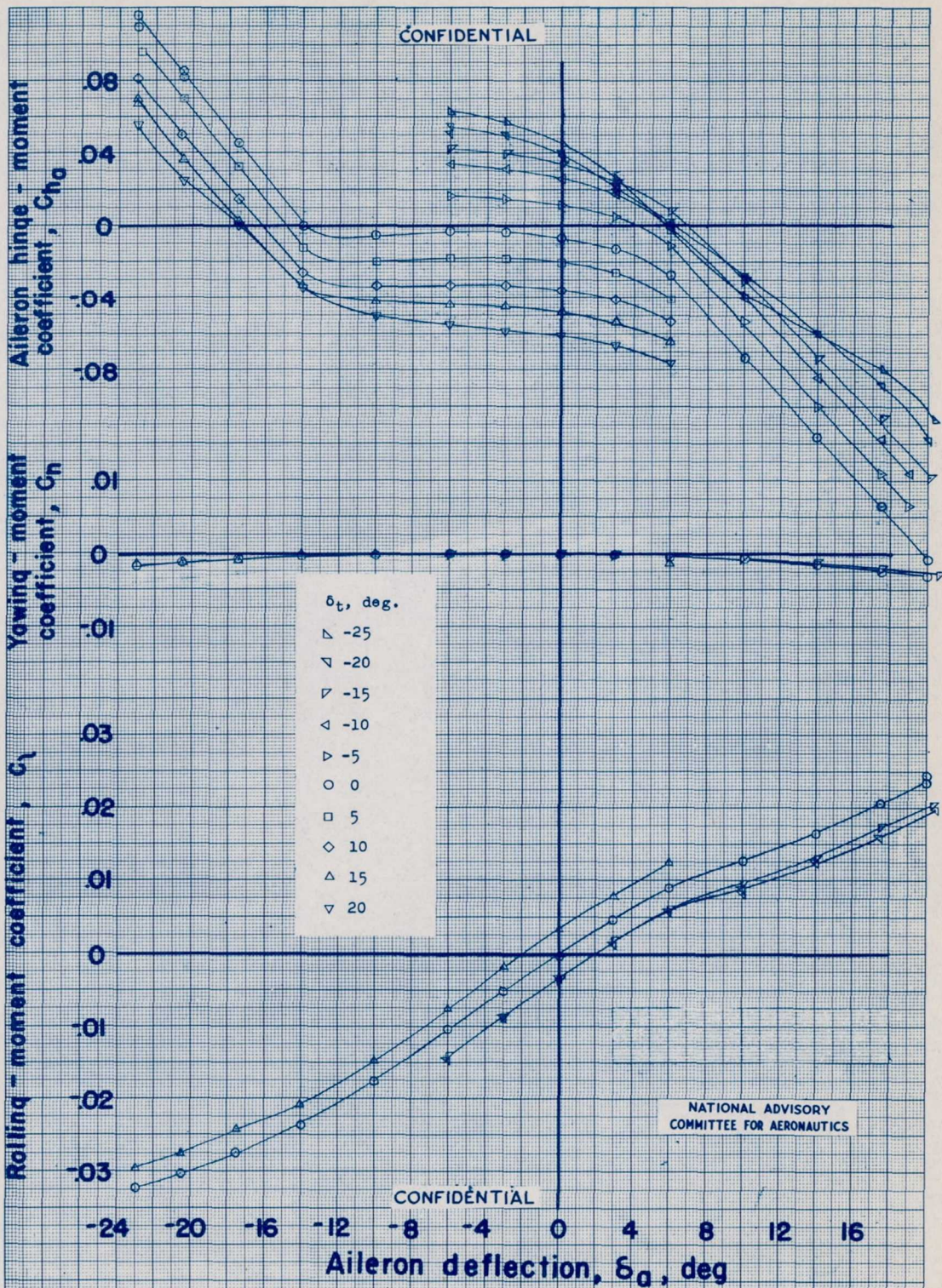
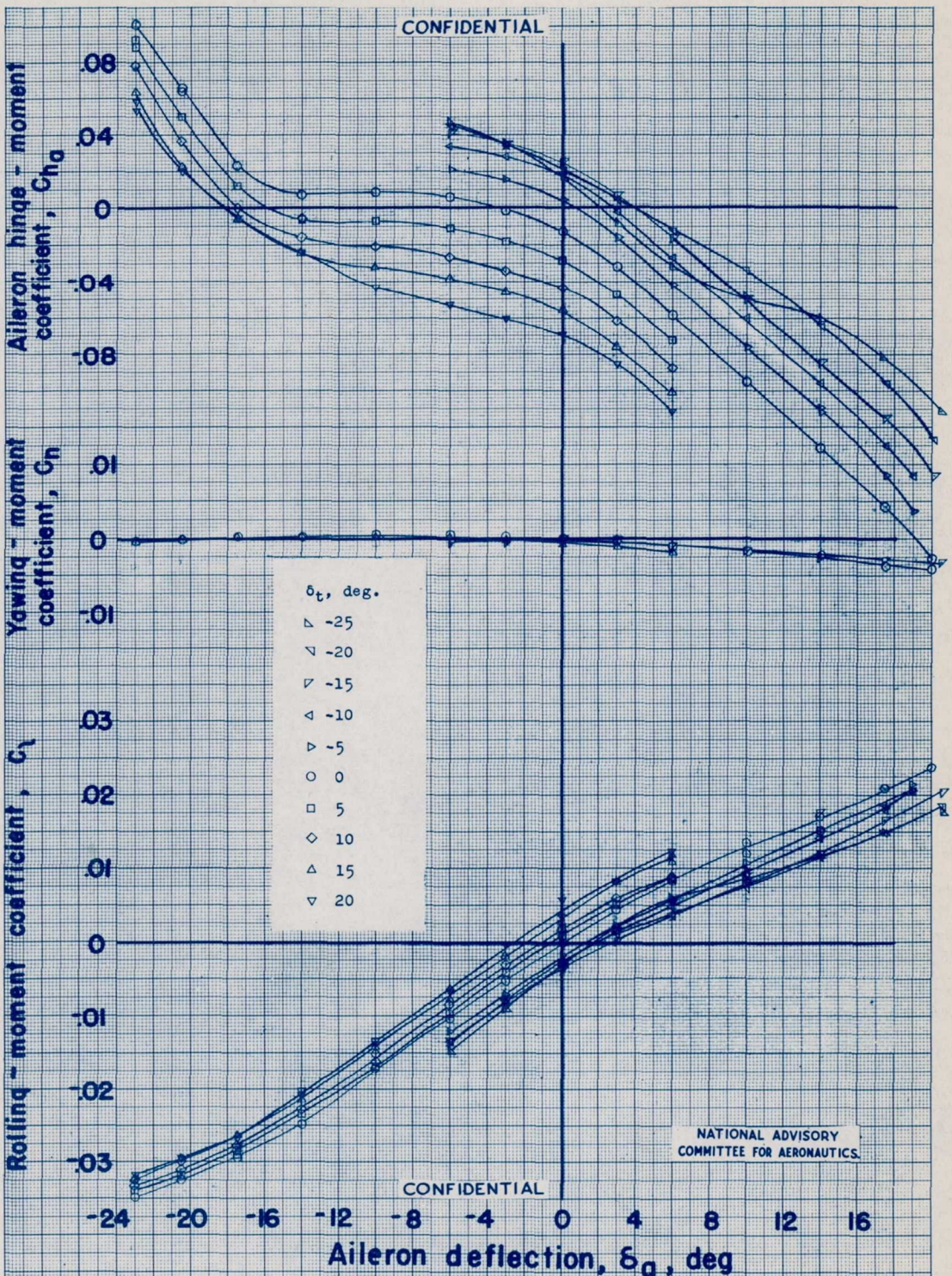


Figure 11.- Aileron and tab characteristics of 1/4-scale partial-span model of the XF-12 airplane. Smooth model; $\delta_f = 55^\circ$; $E = 0.027$.



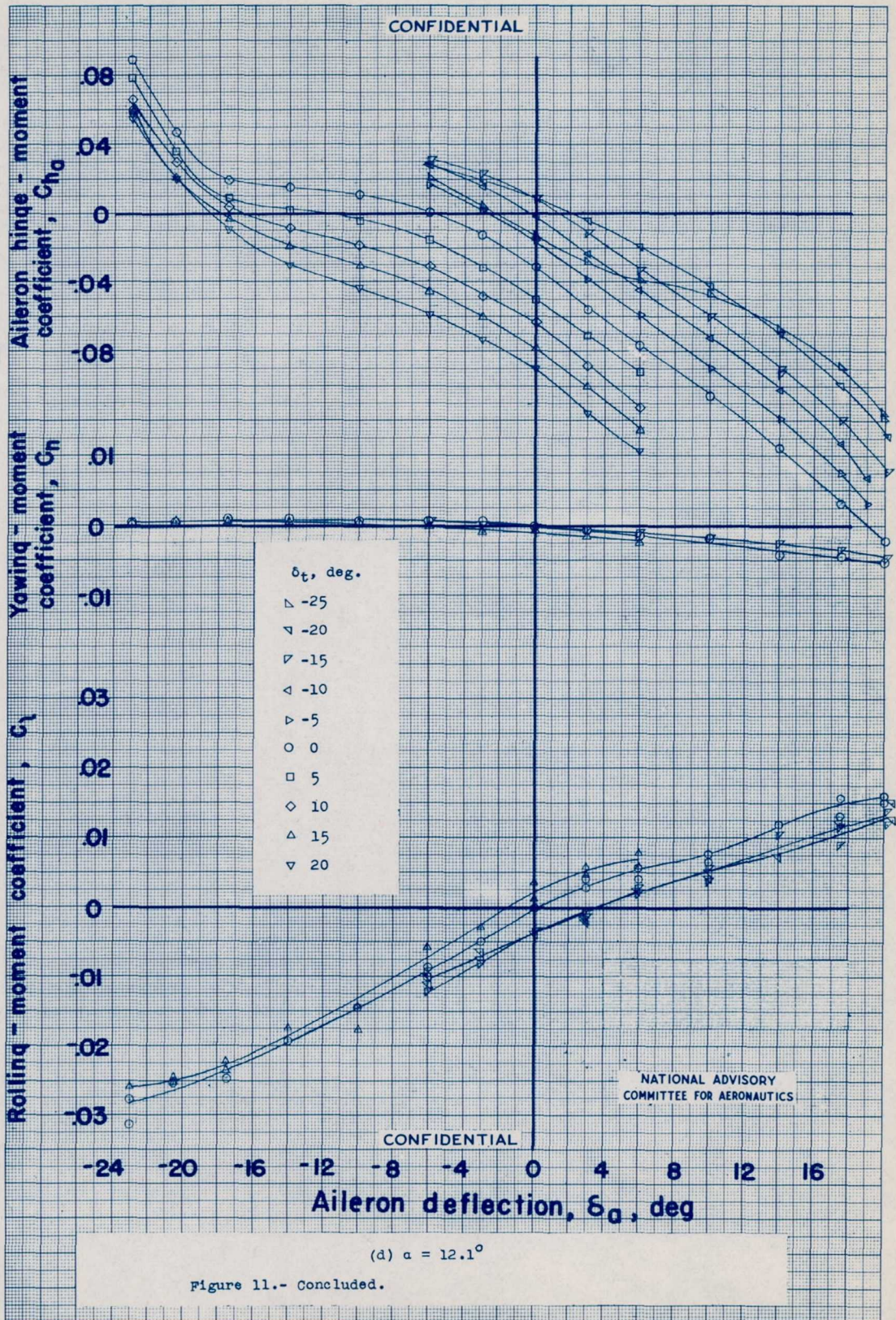
(b) $\alpha = 2.3^\circ$

Figure 11.- Continued.



(c) $\alpha = 7.4^\circ$

Figure 11.- Continued.



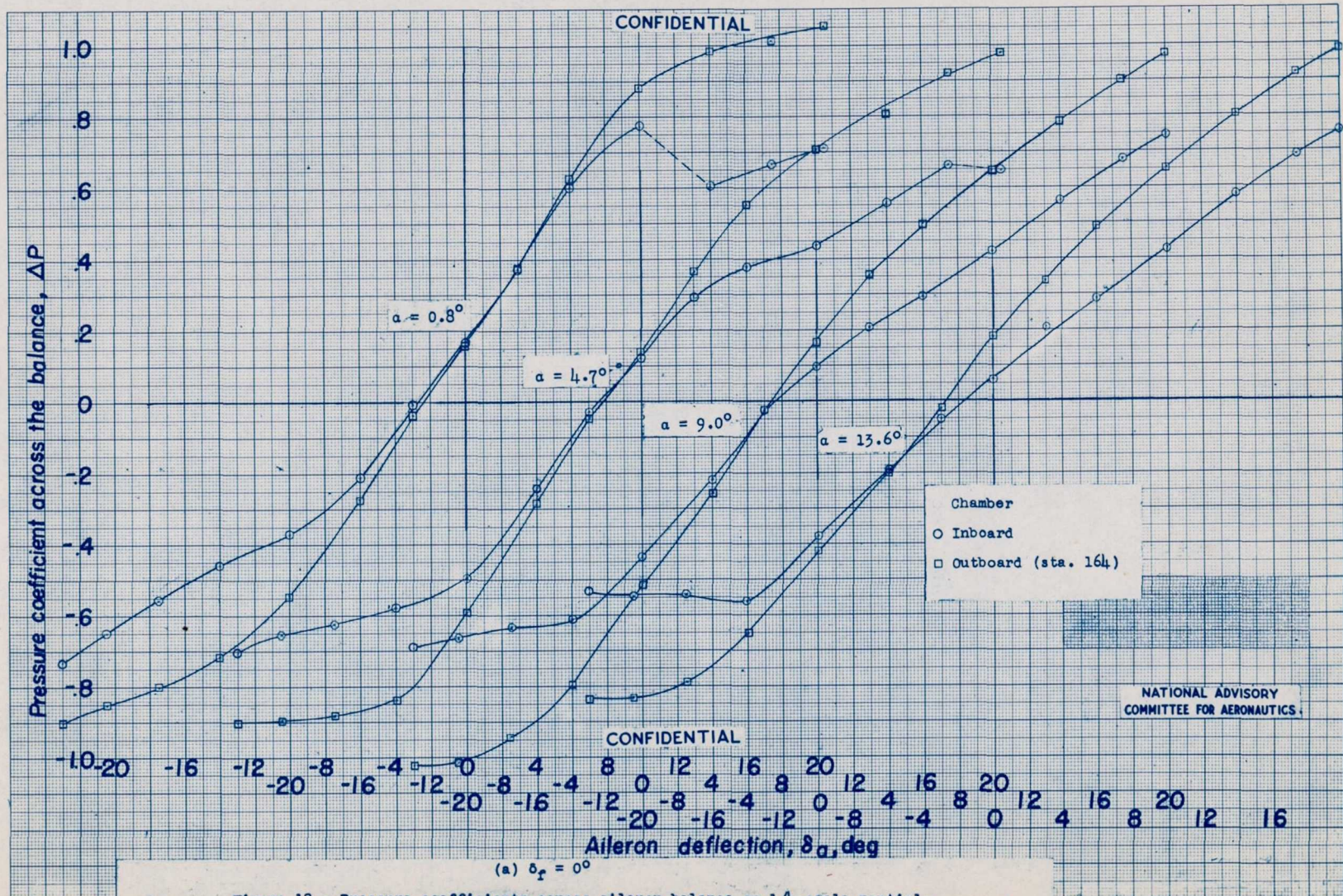


Figure 12.- Pressure coefficients across aileron balance on 1/4-scale partial-span model of the XF-12 airplane. Smooth model; $\delta_r = 0^\circ$; $E = 0.027$.

NATIONAL ADVISORY
COMMITTEE FOR AERONAUTICS.

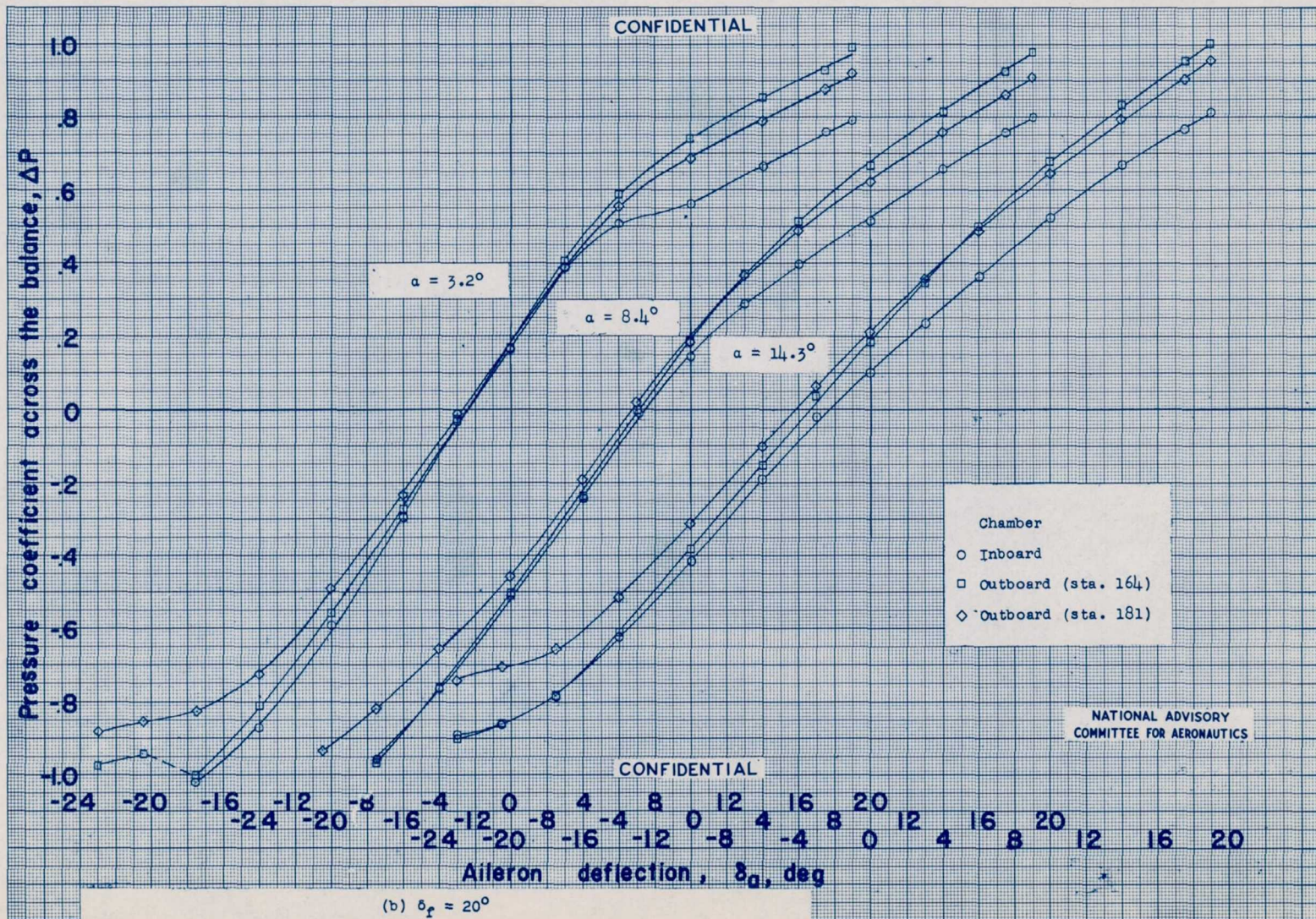


Figure 12.- Continued.

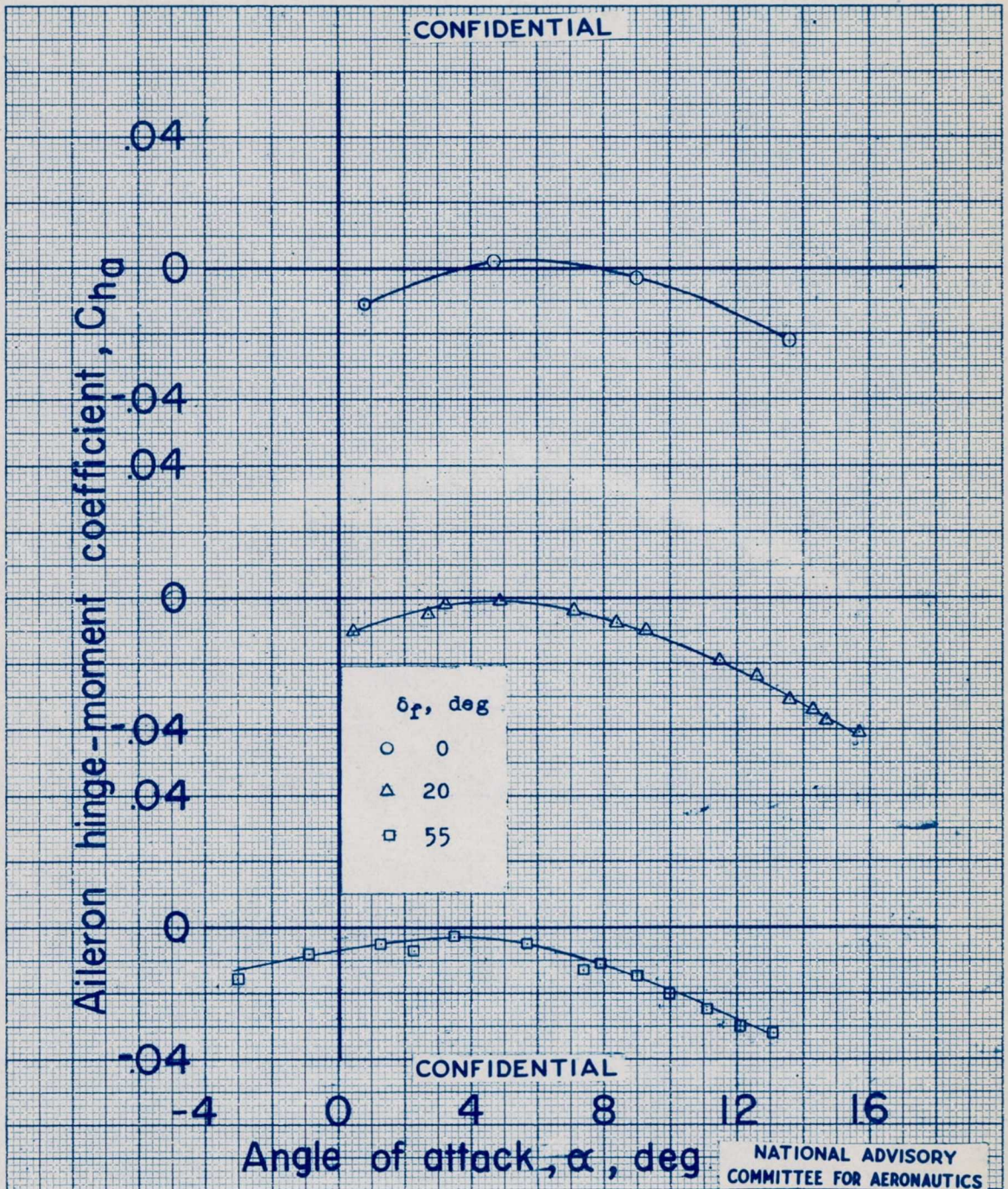


Figure 13.- Variation of aileron hinge-moment coefficient with angle of attack on the 1/4-scale partial-span model of the XF-12 airplane. Smooth model; $\delta_a = 0$; $\delta_t = 0$; $E = 0.027$.

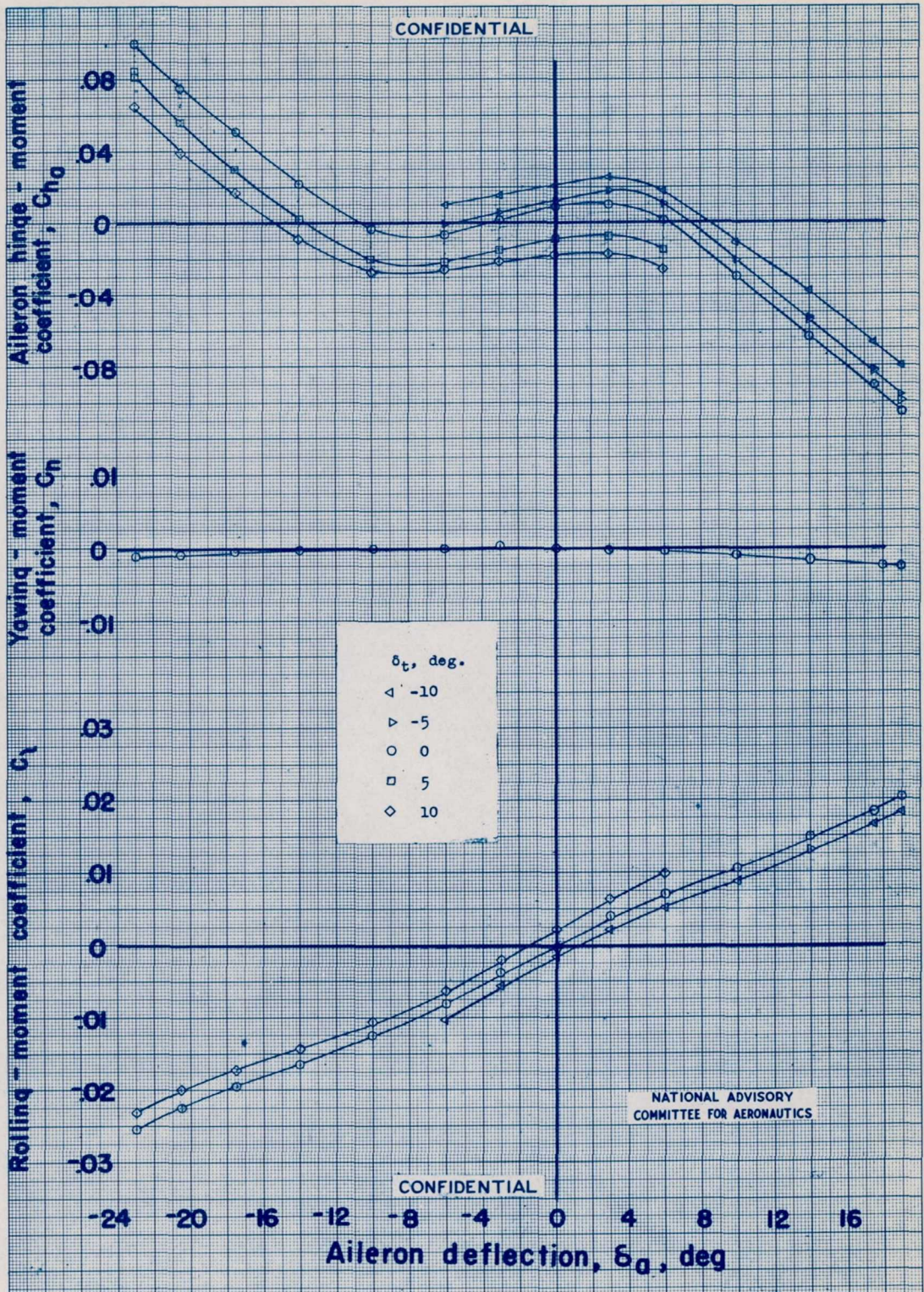


Figure 14.- Aileron and tab characteristics of 1/4-scale partial-span model of the XP-12 airplane. Roughness strips at 0.20c; $\delta_r = 0^\circ$; $\alpha = 0.8^\circ$; $E = 0.027$.

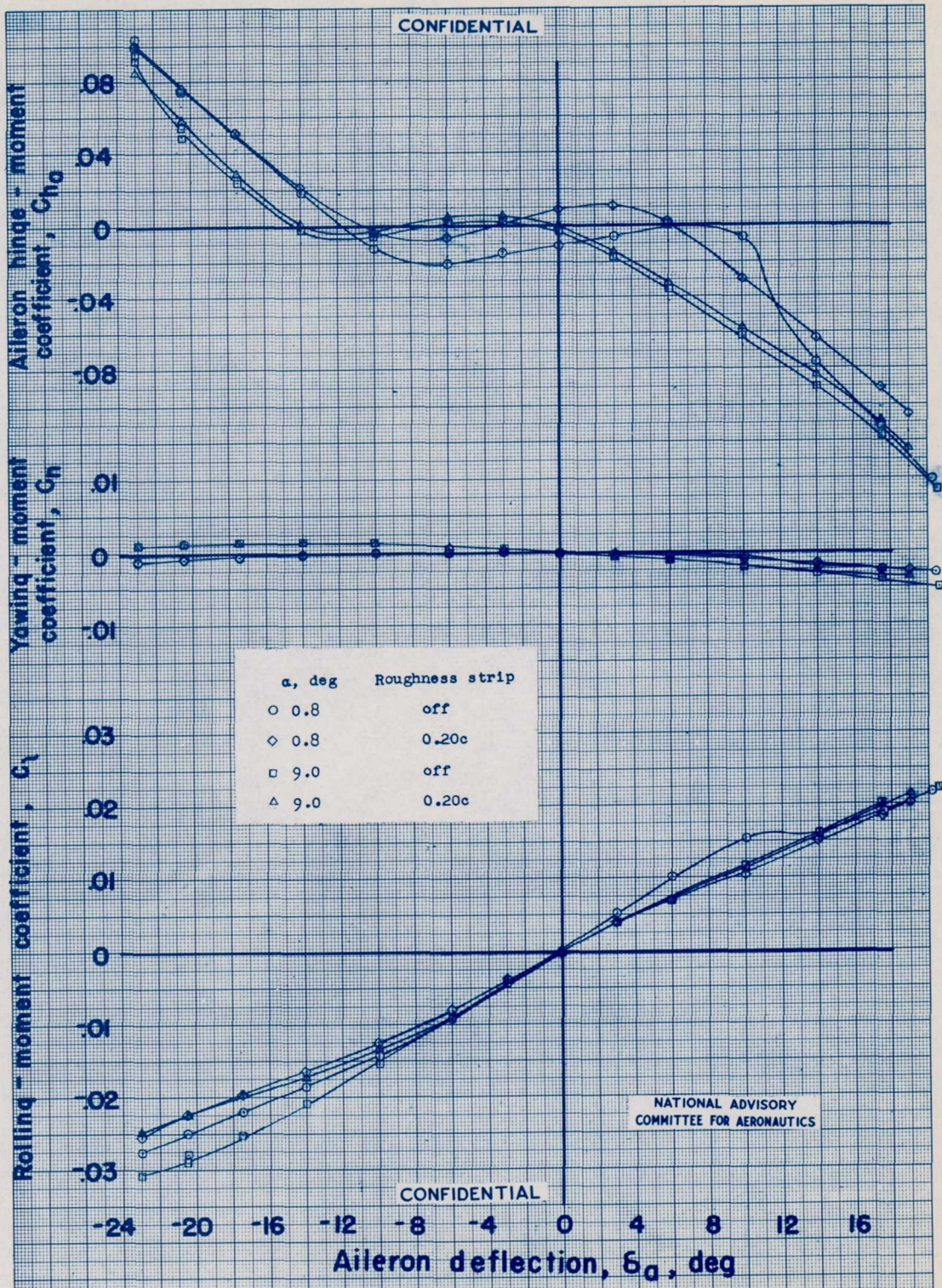


Figure 15.- Effects of roughness strips at 0.20c on aileron characteristics of 1/4-scale partial-span model of the XF-12 airplane. $\delta_r = 0^\circ$; $\delta_t = 0^\circ$; $E = 0.027$.

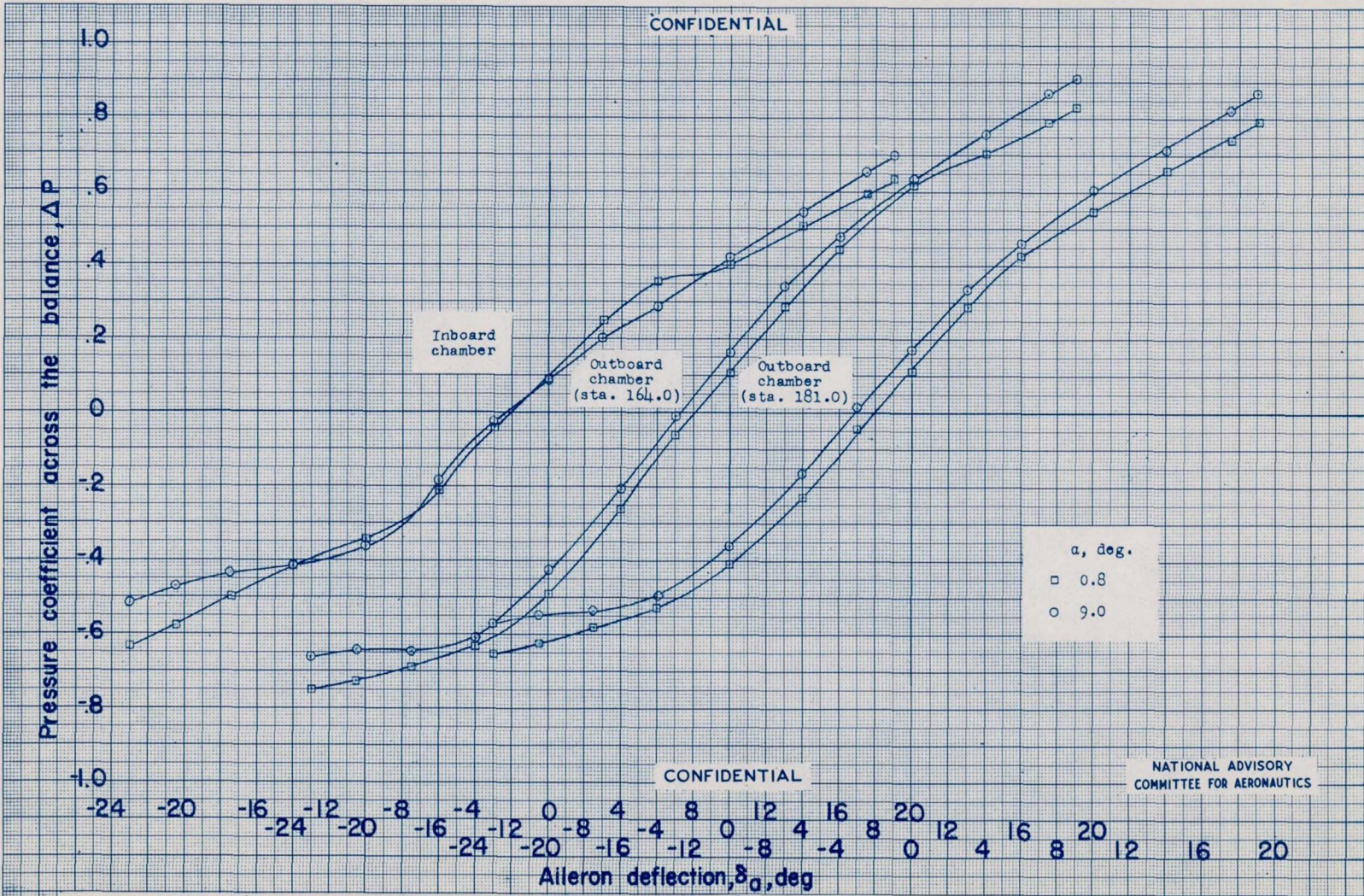
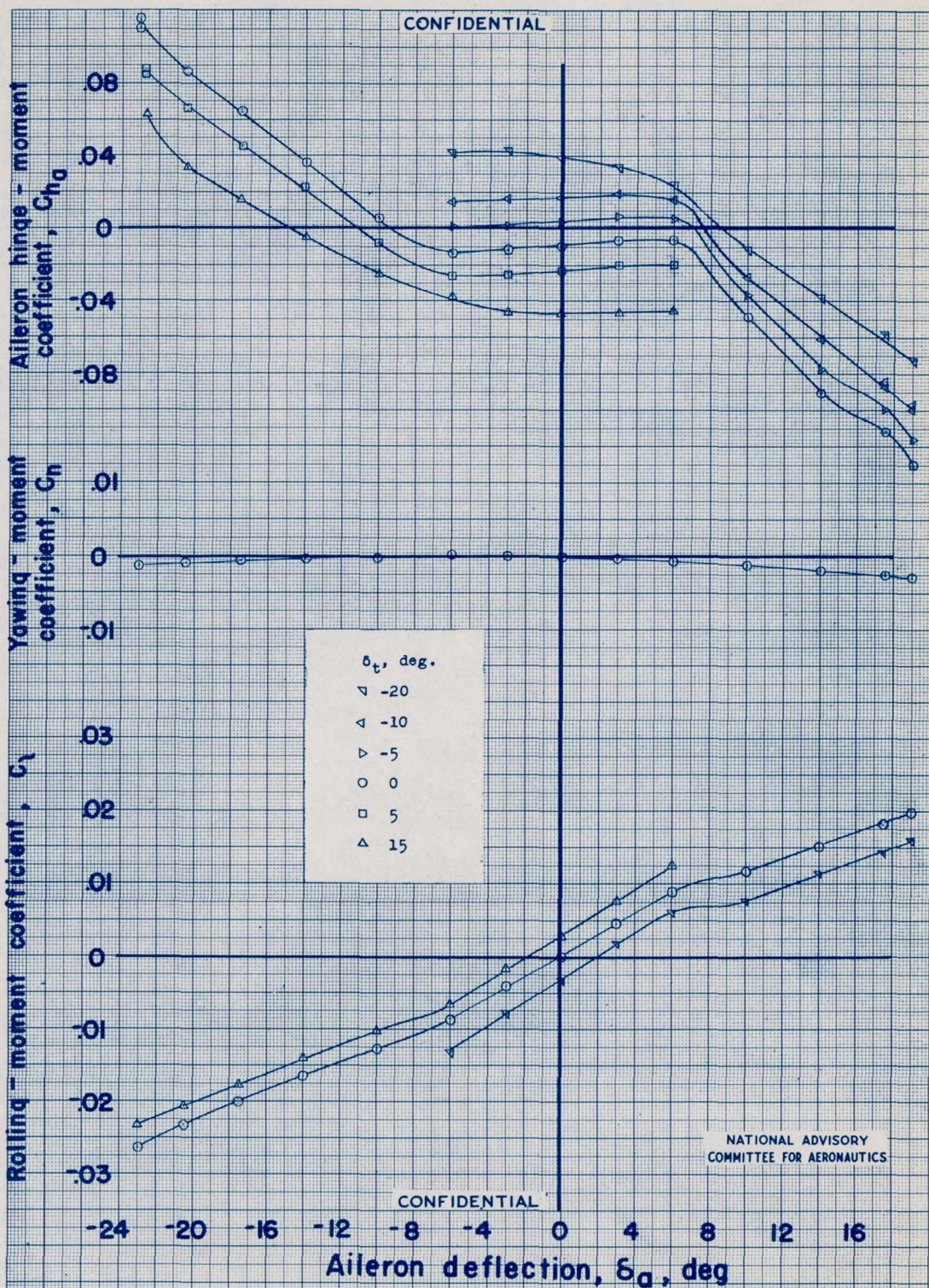
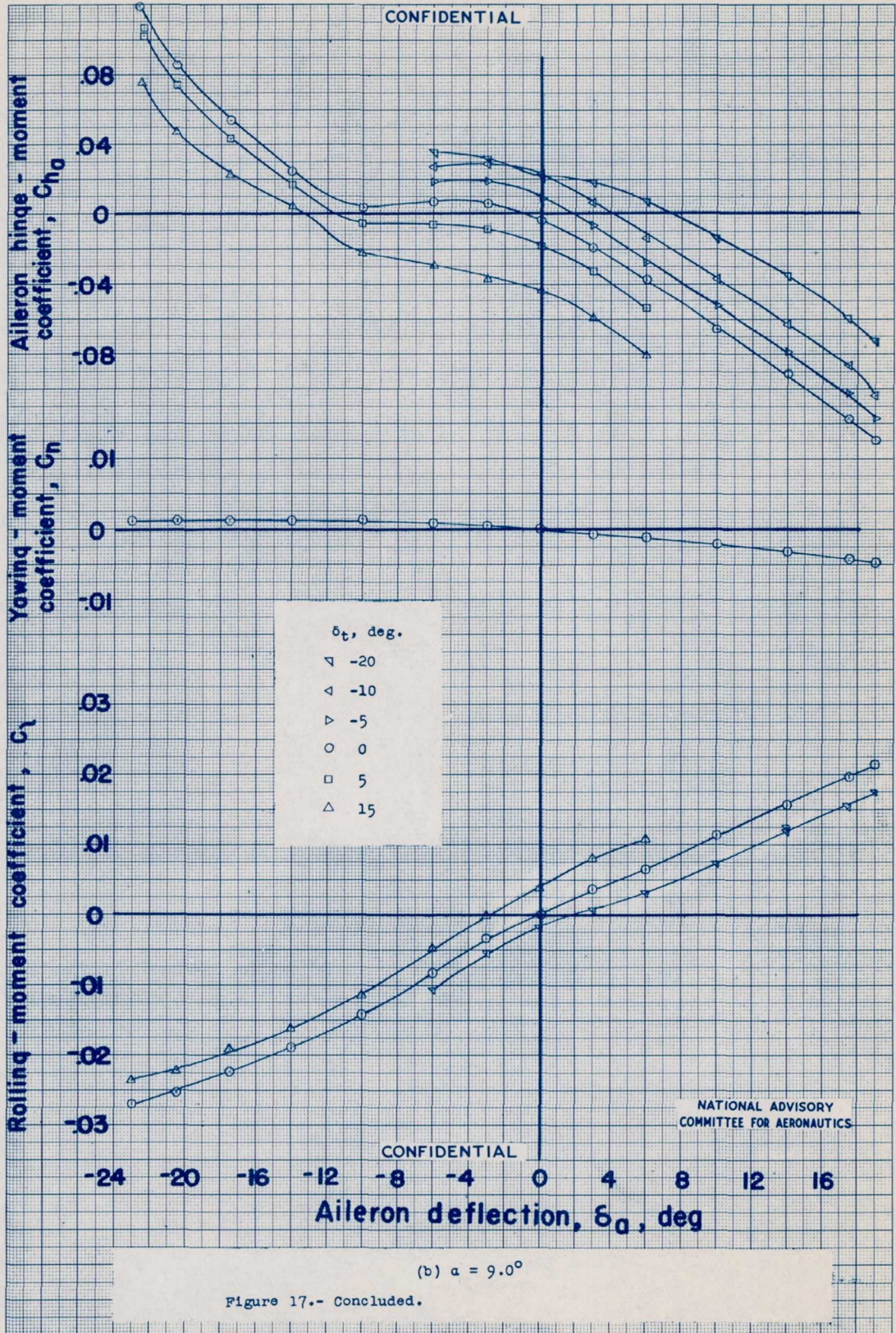


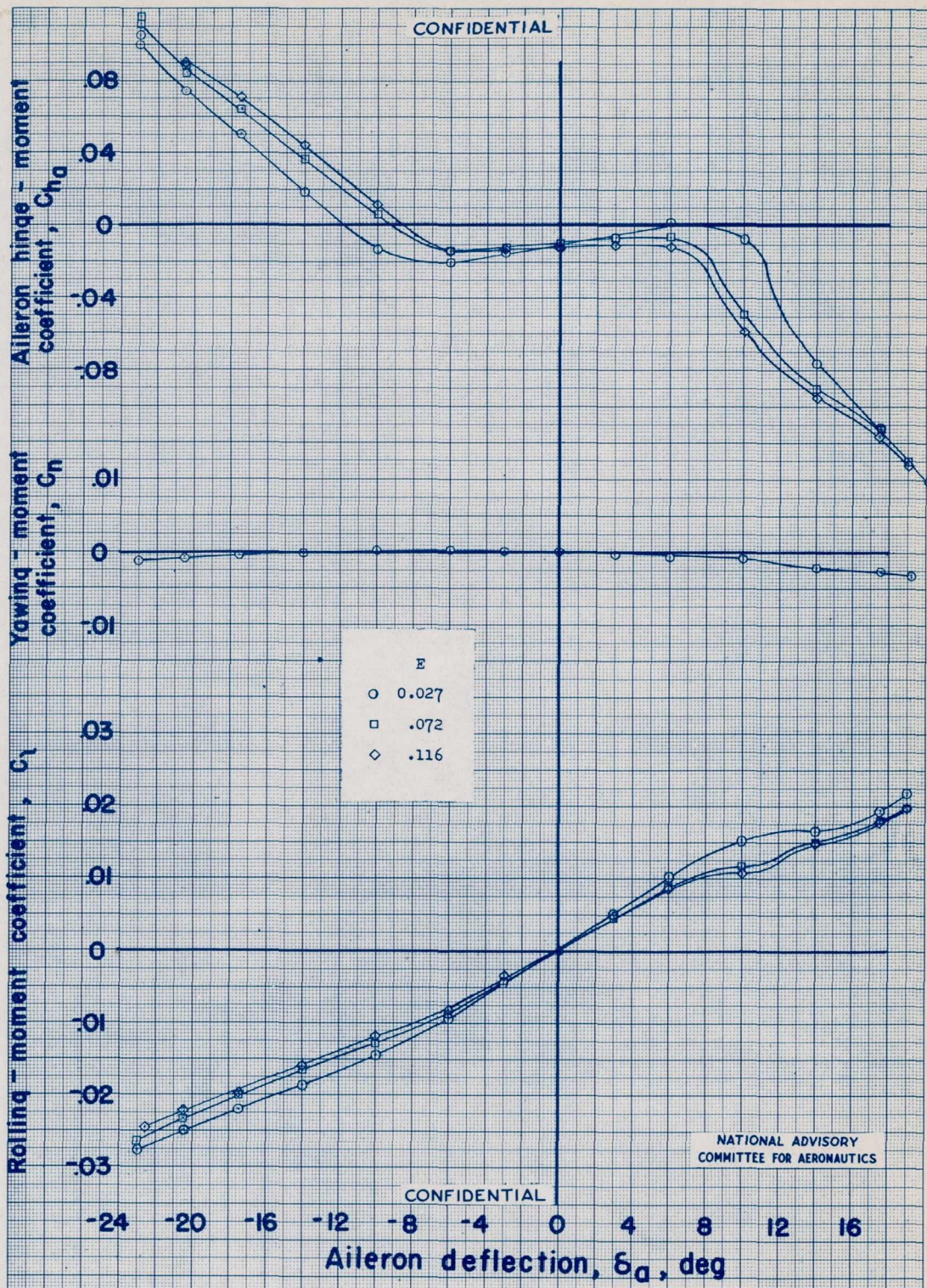
Figure 16.- Pressure coefficients across aileron balance on 1/4-scale partial-span model of the XF-12 airplane. Roughness strips at 0.20c; $\delta_r = 0$; $\delta_t = 0$; $E = 0.027$.



(a) $\alpha = 0.8^\circ$

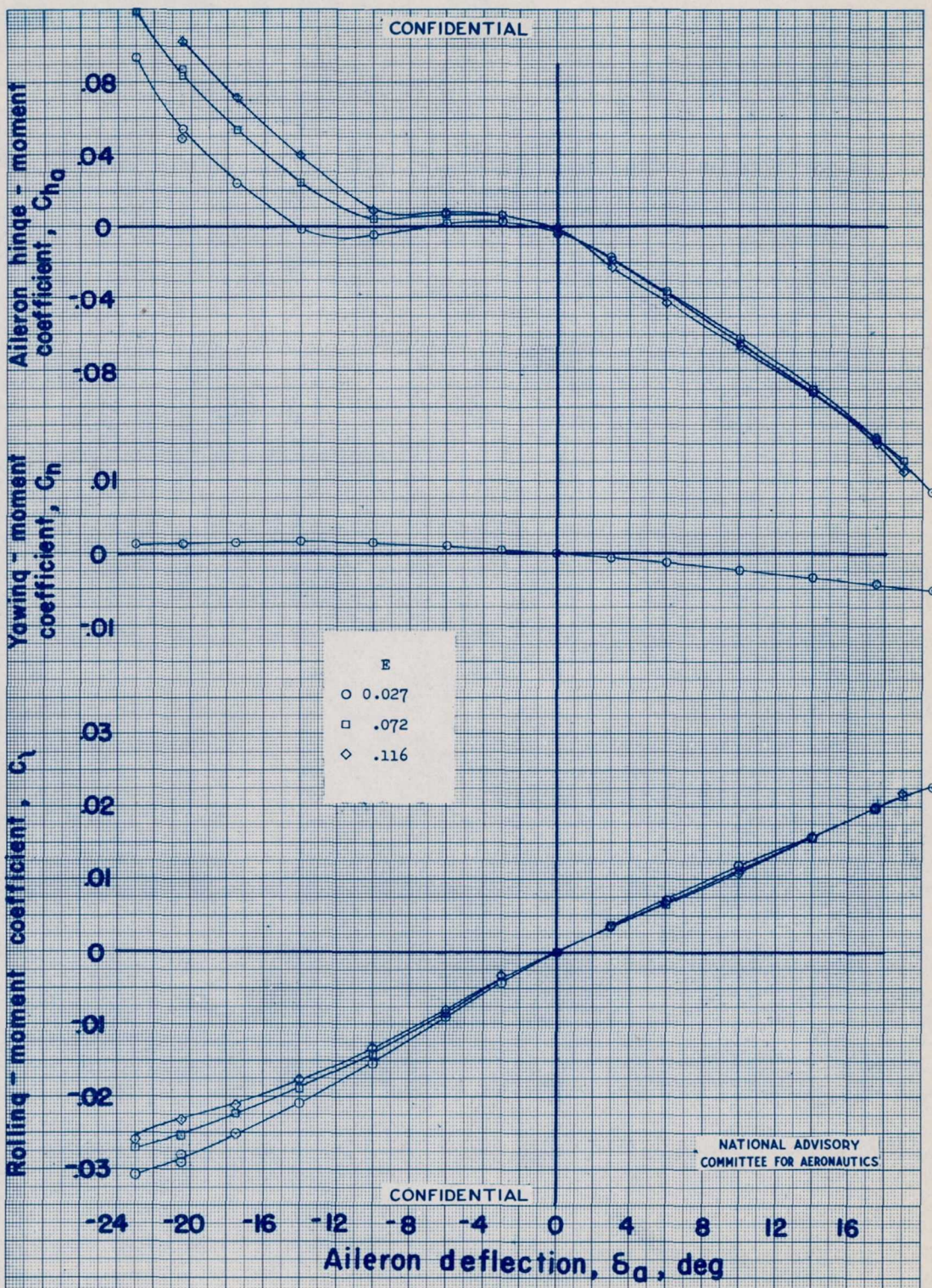
Figure 17.- Aileron and tab characteristics of 1/4-scale partial-span model of the XF-12 airplane. Smooth model; $\delta_r = 0^\circ$; $E = 0.072$.





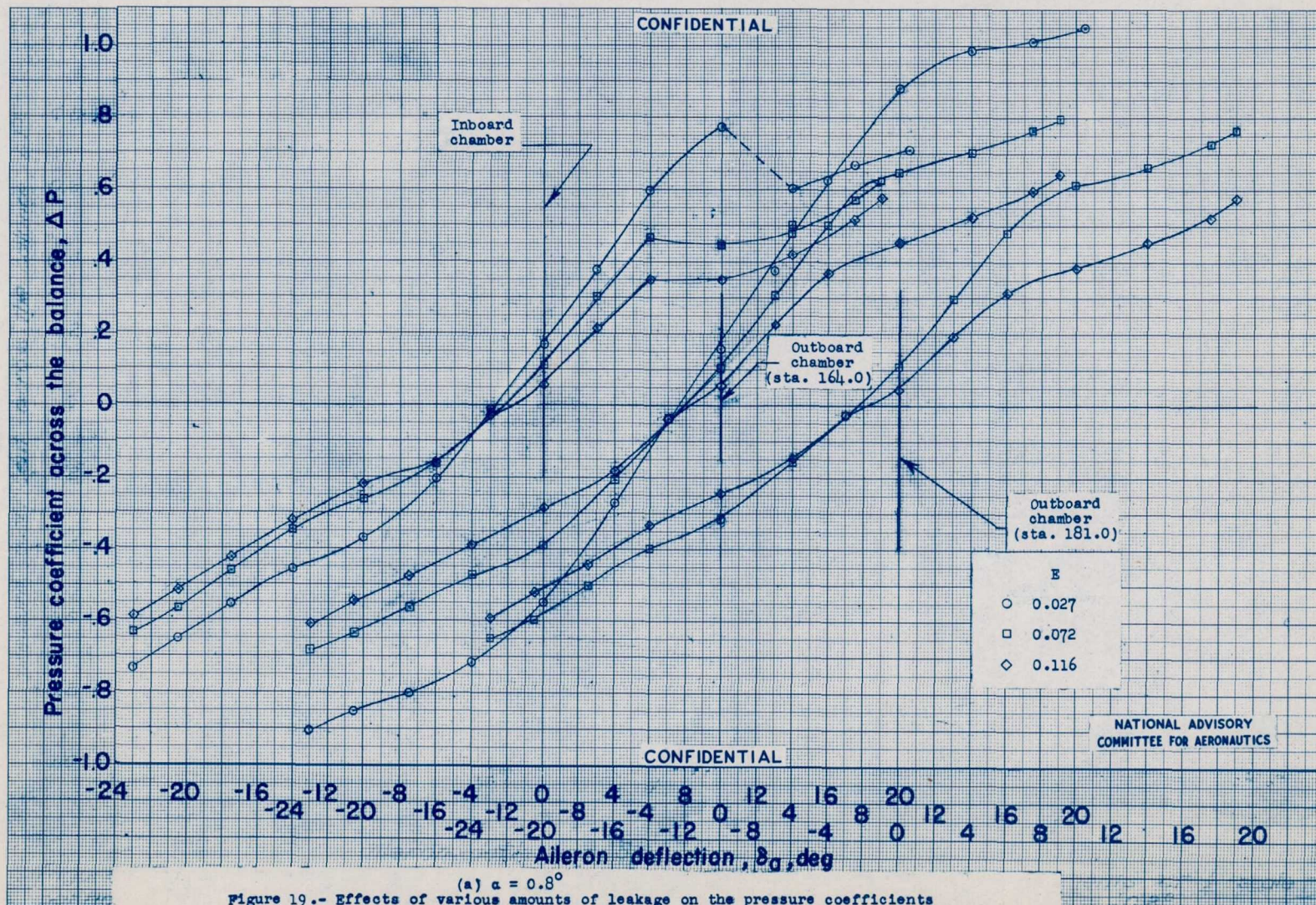
(a) $\alpha = 0.8^\circ$

Figure 18.- Effects of various amounts of leakage on the aileron characteristics of 1/4-scale partial-span model of the XF-12 airplane. Smooth model; $\delta_f = 0^\circ$; $\delta_t = 0^\circ$.



(b) $\alpha = 9.0^\circ$

Figure 18.- Concluded.



(a) $\alpha = 0.8^\circ$
 Figure 19.- Effects of various amounts of leakage on the pressure coefficients across the aileron balance of 1/4-scale partial-span model of the XF-12 airplane. Smooth model; $\delta_f = 0^\circ$; $\delta_t = 0^\circ$.

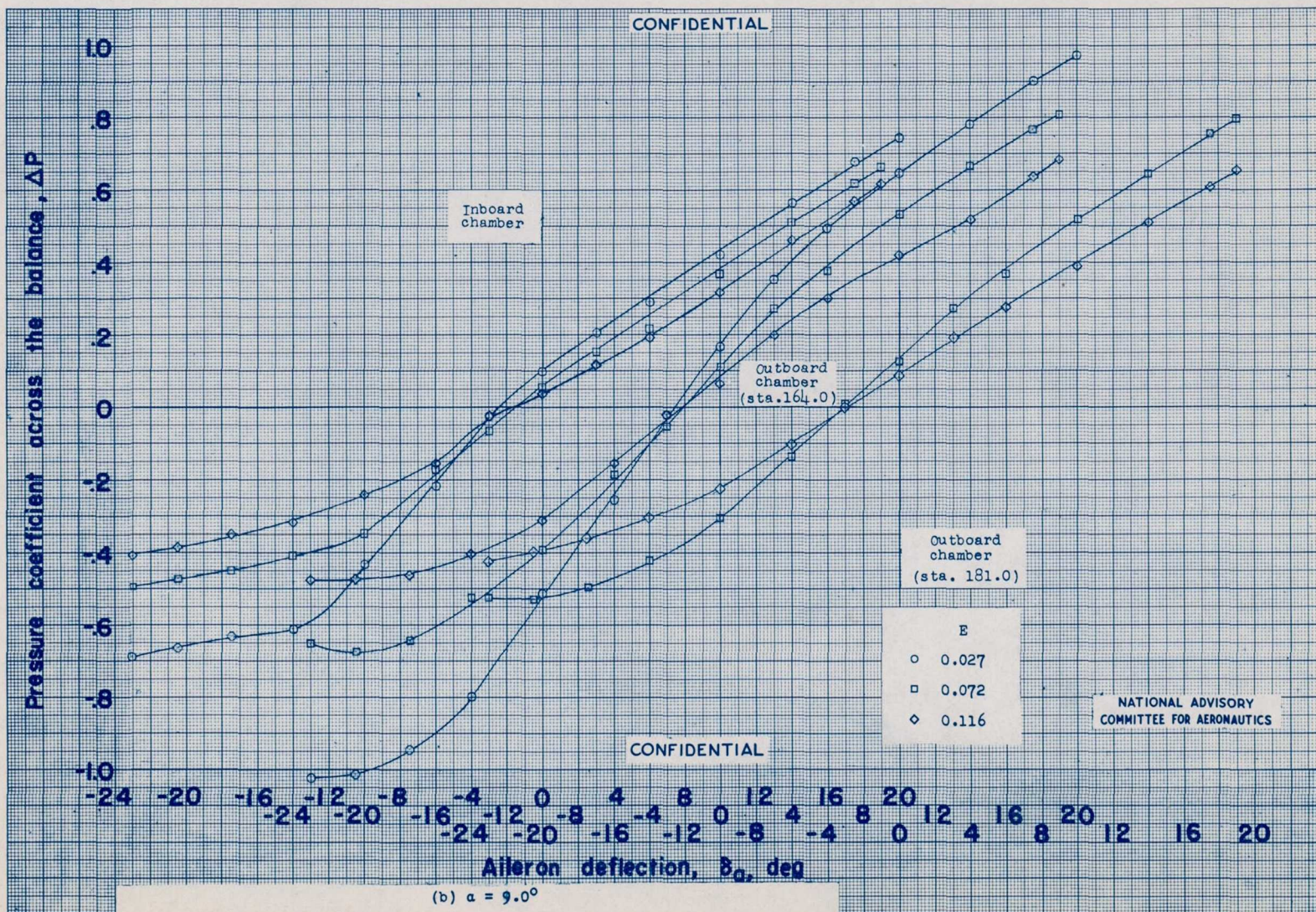
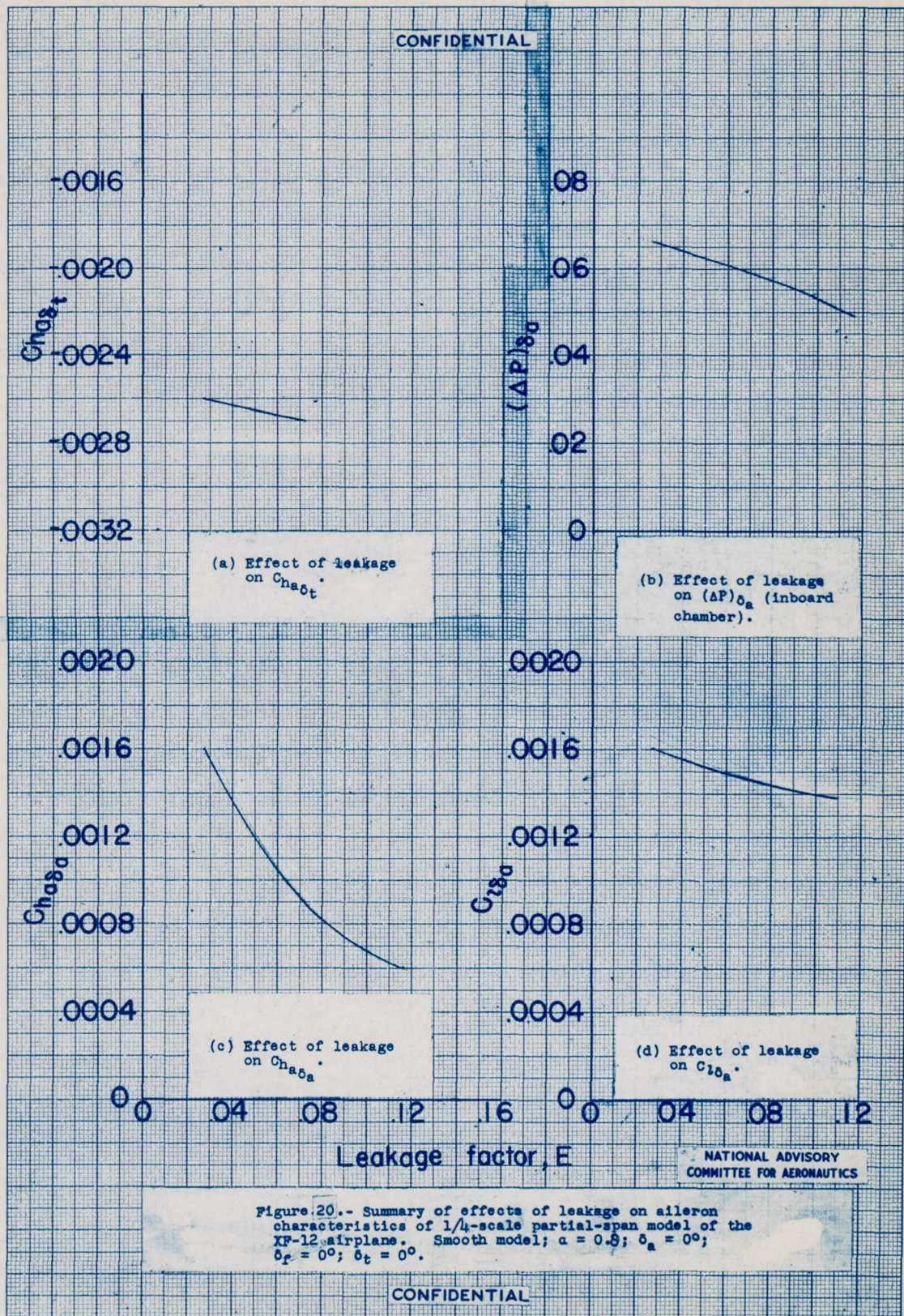
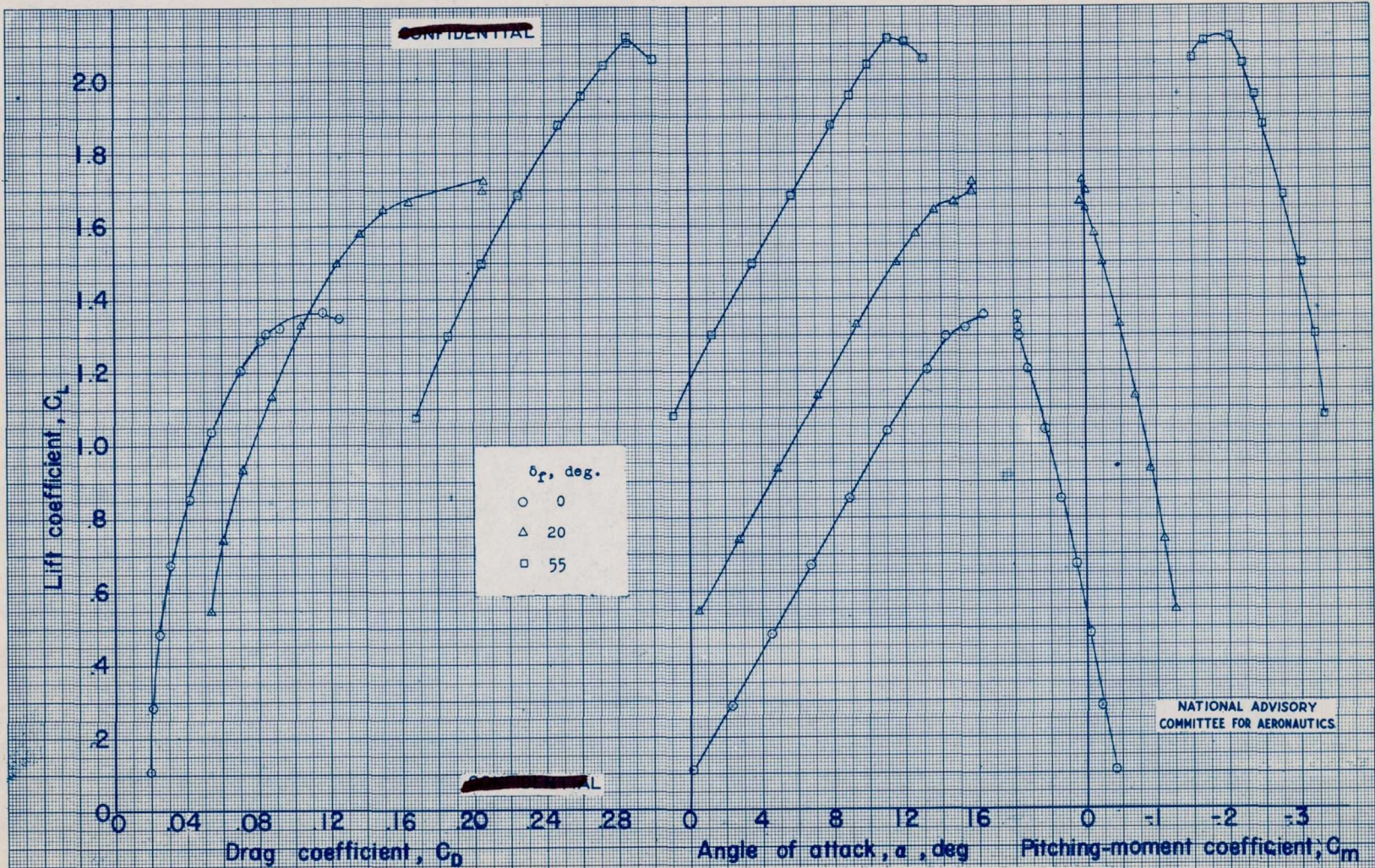


Figure 19.- Concluded.

CONFIDENTIAL





(a) C_L vs C_D , α , and C_m
 Figure 21.- Aerodynamic characteristics of 1/4-scale partial-span model of the XF-12 airplane. $\delta_a = 0^\circ$; $\delta_t = 0^\circ$.